TAMPEREEN TEKNILLINEN YLIOPISTO
TAMPERE UNIVERSITY OF TECHNOLOGY

TUULI SEPPÄNEN

IMPROVING DISTILLATION MODELLING IN A DYNAMIC PROCESS SIMULATOR

Master of Science Thesis

Examiner: Prof. Matti Vilkko
Examiner and topic approved by the Faculty Council of the Faculty of Engineering Sciences on
13th January 2016

ABSTRACT

TUULI SEPPÄNEN: Improving distillation modelling in a dynamic process simulator
Tampere University of Technology
Master of Science Thesis, 66 pages, 5 Appendix pages
August 2016
Master's Degree Programme in Automation Engineering
Major: Process Automation
Examiner: Professor Matti Vilkko

Keywords: dynamic simulation, distillation, tray hydraulics

The need of maximizing the economic benefits of a distillation unit often requires operating close to its capacity limits. The limits of an operating column depend on the internal vapor and liquid flows and their physical properties. In this thesis, distillation modelling in a dynamic process simulator was improved to consider internal phenomena in a distillation column i.e. tray hydraulics.

The structure of the original distillation model was first reconsidered. In the developed model, separate flash separators were used to represent an active area and a downcomer of a tray. The hydraulic phenomena included in the model were jet flooding, downcomer backup flooding, downcomer choke flooding and weeping. Downcomer backup flooding occurred in the model automatically due to the model structure and configuration. To represent the other hydraulic phenomena in the model, correlations were used. These correlations were rationalized based on the literature study. For determining the limit values, at which each phenomenon begins, and maximum jet flooding and downcomer choke flooding occurs in a specific distillation column, Koch-Glitsch's KG-TOWER software was utilized.

The developed distillation model was first implemented in the dynamic process simulator with fixed pressure, and jet flooding, downcomer choke flooding and weeping occurring only on one tray. The liquid flow rates, pressures and levels of the tanks were also calculated manually with a spreadsheet, and simulation results were compared to those to verify the accuracy of the simulation model. After ensuring the reasonable function of the correlations, the calculation of the correlations was implemented in the simulator code by programming. For more extensive examination, the model was implemented in a distillation game model. The function of the model was studied by varying the reboiler duty, feed rate and reflux rate.

The simulation results showed that some oscillation occurs easily both in flooding and in weeping. To ensure the stability in all situations, the model configuration needs further examination. All the hydraulic phenomena did, however, occur in the model according to implemented calculation as assumed.

TIIVISTELMÄ

TUULI SEPPÄNEN: Dynaamisen prosessisimulaattorin tislausmallin kehittäminen
Tampereen teknillinen yliopisto
Diplomityö, 66 sivua, 5 liitesivua
Elokuu 2016
Automaatiotekniikan diplomi-insinöörin tutkinto-ohjelma
Pääaine: Prosessien hallinta
Tarkastaja: Professori Matti Vilkko

Avainsanat: dynaaminen simulointi, tislaus, välipohjahydrauliikka

Tislauskolonnin taloudellisten hyötyjen maksimoiminen vaatii usein kolonnin operoimista lähellä sen kapasiteettirajoja. Nämä rajat riippuvat kolonnin sisäisistä kaasu- ja nestevirtauksista sekä niiden fysikaalisista ominaisuuksista. Tässä diplomityössä kehitettiin dynaamisen prosessisimulaattorin tislausmallinnusta siten, että se ottaa huomioon tislauskolonnin sisäiset ilmiöt eli välipohjahydrauliikan.

Ensimmäisenä alkuperäisen tislausmallin rakennetta harkittiin uudelleen. Kehitetyssä mallissa käytettiin erillisiä sekoitussäiliöitä kuvaamaan välipohjan aktiivialuetta ja paluukaukaloa. Työssä mallinnetut hydrauliset ilmiöt olivat roiskinta, paluukaukalon tulviminen sekä itkeminen. Paluukaukalon tulviminen johtuen nesteen ajautumisesta aktiivialueelta takaisin paluukaukaloon tapahtui mallissa sen rakenteen ja konfiguraation vuoksi automaattisesti. Muiden hydraulisten ilmiöiden kuvaamiseen käytettiin korrelaatioita. Korrelaatioiden määrittämisessä hyödynnettiin työn kirjallisuusosan selvitystä. Kunkin ilmiön alkamisen ja maksimitulvimisen raja-arvojen määrittämisessä tietylle kolonnille käytettiin Koch-Glitsch KG-TOWER -ohjelmistoa.

Kehitetty tislausmalli rakennettiin ensin dynaamiseen prosessisimulaattoriin vakiopaineella ja siten, että roiskinta, paluukaukalon tulviminen ja itkeminen tapahtuivat vain yhdellä välipohjalla. Nestevirtaukset, paineet ja säiliöiden pinnankorkeudet laskettiin myös taulukkolaskentaohjelmalla, ja simulointituloksia verrattiin laskujen tuloksiin simulointimallin tarkkuuden verifioimiseksi. Kun korrelaatioiden toiminta varmistettiin järkeväksi, korrelaatioiden laskenta implementoitiin simulaattoriin ohjelmoimalla. Laajempaa tutkimista varten mallia sovellettiin tislauspelimalliin. Mallin käyttäytymistä tutkittiin vaihtelemalla kiehuttimen tehoa sekä syötön ja huipunpalautuksen määrää.

Simulointitulokset osoittivat, että mallissa esiintyy helposti oskillointia sekä tulvimisen että itkemisen aikana. Mallin konfiguraatio tarvitsee lisää tarkastelua, jotta mallin stabiilius voidaan taata kaikissa tilanteissa. Kaikki hydrauliset ilmiöt esiintyivät kuitenkin mallissa toteutetun laskennan mukaan, kuten oletettiin.

PREFACE

This master's thesis was done for the Department of Technology and Product Development at Neste Jacobs in Porvoo during the 1st of November 2015 and the 30th of April 2016. This thesis was accomplished in co-operation with Neste.

First of all, I want to thank M.Sc. Jyri Lindholm and M.Sc. Esa Tamminen for giving me this opportunity to work with such an interesting thesis. I am also very grateful to Esa Tamminen for all the guidance he gave me throughout the process as an advisor at Neste. I would also like to express my gratitude to my advisors at Neste Jacobs. I want to thank M.Sc. Tanja Granholm for always finding the time to help me. To M.Sc. Teemu Liikala I am grateful for the invaluable guidance he gave me about the software. I greatly appreciate the whole Dynamic Simulation team at Neste Jacobs for providing a great environment to work in. In addition, I want thank the examiner of this thesis Prof. Matti Vilkko for the helpful feedback he gave me.

My warmest thanks go to my family and friends for encouraging me during this process as well as the whole studies. I want to thank my parents for the support they have given me with studies and life. My sister, brother and friends I want to thank for providing the enjoyable counterbalance to studies and work. Fellow students and friends also deserve thanks, especially Sanna, I would like to thank you for being such a great friend to study with and for all the peer support you have given during the whole university studies. Last but not least, I want to thank my dearest Teemu for always being there for me.

In Porvoo, on 12 June 2016

Tuuli Seppänen

CONTENTS

LIST OF SYMBOLS AND ABBREVIATIONS

PR	Peng-Robinsin equation of state
SRK	Soave-Redlich-Kwong equation of state
VLE	Vapor-liquid equilibrium
A_{apron}	Area of downcomer apron, m2
A_a	Active tray area, m2
C_d	Discharge coefficient, -
CF	Capacity factor, m/s
CF_0	Capacity factor at zero liquid load, m/s
d_h	Hole diameter, m
$E_{i,n}$	Murphree tray vapor efficiency for component *n* in tray *i*, -
F_i	Feed molar flow to tray *i*, mol/h
g	Acceleration of gravity, m/s^2
H_i	Enthalpy of vapor phase leaving tray *i*, J/mol
H_{i+1}	Enthalpy of vapor phase coming to tray *i*, J/mol
h_{cl}	Clear liquid height on tray, m
h_{cli}	Clear liquid height at liquid entry in downcomer, m
h_{dc}	Liquid height in downcomer, m
h_f	Enthalpy of feed, J/mol
h_{fd}	Froth height in downcomer, m
h_i	Enthalpy of liquid phase leaving tray *i*, J/mol
h_{i-1}	Enthalpy of liquid phase coming to tray *i*, J/mol
h_n	Pressure increase across nappe, m of liquid
h_{udc}	Pressure drop for flow under downcomer, m of liquid
h_t	Total pressure drop, m of liquid
h_1	Clearance under downcomer, m
$K_{i,n}$	Equilibrium constant for component *n* in tray *i*, -
L	Characteristic length, m
L_{att}	Liquid amount attempting to flow to downcomer, t/h
L_{choke}	Liquid flow rate from active area to downcomer, t/h
L_i	Liquid molar flow leaving tray *i*, mol/h
L_{i-1}	Liquid molar flow coming to tray *i*, mol/h
L_{jet}	Liquid entrainment rate, t/h
L_{lim}	Liquid flow at which choke flow is first limited, t/h
$L_{max,choke}$	Liquid flow at which maximum limitation of choke flow occurs, t/h
$L_{max,jet}$	Maximum liquid entrainment rate, t/h
$L_{max,weep}$	Maximum liquid weeping rate, t/h
L_{weep}	Weeping liquid rate, t/h
$M_{i,n}$	Total molar holdup of component *n* in tray *i*, mol
M_i	Total molar holdup in tray *i*, mol
$M_i h_i$	Molar holdup of the liquid phase enthalpy in tray *i*, J
P_i	Total pressure in tray *i*, kPa
$P_{i,n}^0$	Vapor pressure of component *n* in pure liquid phase in tray *i*, kPa

PL_i	Liquid product flow, mol/h
PV_i	Vapor product flow, mol/h
Δp_{tray}	Pressure drop over tray, kPa
Δp_{static}	Liquid head on tray, kPa
Δp_{dry}	Dry pressure drop, kPa
Δp_r	Residual pressure drop, kPa
Q_i	Heat input to tray *i*, W
Q_L	Liquid flow rate, m^3/s
Q_t	Liquid flow under downcomer, m^3/s
Q_V	Vapor flow rate, m^3/s
SF	System factor, -
v_{dc}	Velocity under the downcomer apron, m/s
v_h	Vapor velocity through hole, m/s
V_i	Vapor molar flow leaving tray *i*, mol/h
V_{i+1}	Vapor molar flow coming to tray *i*, mol/h
$V_{lim,jet}$	Vapor rate at which jet flooding starts to occur, t/h
$V_{lim,weep}$	Vapor rate at which weeping starts to occur, t/h
$V_{max,jet}$	Vapor rate at which maximum jet flooding occurs, t/h
v_V	Superficial vapor velocity, m/s
W	Weir length, m
x_F	Mole fraction of the component *n* in feed, -
$x_{i,n}$	Mole fraction of component *n* in liquid phase leaving tray *i*, -
$x_{i-1,n}$	Mole fraction of component *n* in liquid phase coming to tray *i*, -
$y_{i,n}$	Mole fraction of component *n* in vapor phase leaving tray *i*, -
$y_{i+1,n}$	Mole fraction of component *n* in vapor phase coming to tray *i*, -
$y^*_{i.n}$	Vapor mole fraction of component *n* leaving tray *i* in equilibrium, -
$\bar{\alpha}_d$	Mean liquid volume fraction in downcomer, -
$\gamma_{i,n}$	Liquid activity coefficient of component n, -
ζ	Resistance coefficient, -
ξ	Orifice coefficient, -
ρ_L	Liquid mass density, kg/m^3
ρ_V	Vapor mass density, kg/m^3
σ	Surface tension, N/m
ϕ_n	Vapor fugacity coefficient, -

1. INTRODUCTION

Distillation is one of the most widely used unit operations in the chemical industry [1]. Distillation is a process in which a liquid or vapor mixture is separated into its component fractions by utilizing different volatilities of the components. In a distillation column the more volatile, or lighter, components are removed from the top of the column and the less volatile, or heavier, components are removed from the lower part of the column. The reboiler vaporizes some of the liquid from the base of the column and vapor flows upwards in the column. The condenser liquefies vapor and liquid flows downward in the column. To provide the vapor-liquid contacting, there are either trays or packings in the column.

Distillation operations consume vast amounts of energy. Consequently, great economic savings can be achieved with relatively modest energy saving. The energy consumption of the distillation can be affected by constructional design of the column and the mode of operation. The choice of column internals creates frames for energy consumption and thus defines the lower limit of energy consumption. Nevertheless, efficient operation of the distillation column can significantly affect its energy consumption. [2, p. 1] For a distillation column to operate efficiently, not only must it be well-designed, but the control strategies must be effective to ensure that controlled variables remain at set point in the presence of disturbances that frequently occur in industrial situations.

Simulators are essential appliances for today's process designers. They can be divided into two groups: steady-state and dynamic simulators. Steady-state simulation calculates the state of a stable system whereas dynamic simulation models the behavior of a system over time. With dynamic simulation the behavior of a distillation column can be studied especially in shut-down, start-up and upset situations. In Neste there are several operator training simulator environments in use. More realistic dynamic behavior of the modelled system provides opportunities for developing the training possibilities. This again helps operators to avoid disturbances and to operate the process faster to normal condition in unusual situations.

1.1 Problem of current distillation model

The need of maximizing the economic benefits of a distillation unit very often requires operating close to its capacity limits. The limits of an operating column depend on the internal vapor and liquid flows and their physical properties. [3, p. 131] The process of vapor flowing up the column and liquid flowing across each tray and down the column is called tray hydraulics. It imposes constraints on the range of permissible vapor and

liquid flow rates. [4, p. 29] If the high limit is exceeded, the column may reach unacceptable condition and can no longer be operated. In the low-limit conditions the column can still be operated but with an unacceptable loss of efficiency. [3, p. 132]

As the operation of the distillation column is poor if the vapor or liquid flow rate limit is exceeded, it is important for operators to recognize when the operation approaches these limits. This way the distillation column can be operated as efficiently and economically as possible. In this matter, the operator training simulators can be profitable, if the distillation model in operator simulators can realistically model the operation of the distillation column in limit conditions.

The distillation model utilized in the operator training simulators is modelled with a dynamic process simulator called NAPCON ProsDS. It is software developed by Neste Jacobs and programmed in ANSI Common Lisp. Development of the first version started in 1987 and the software is being continuously improved and extended. [5] In ProsDS there are number of unit models available. The current model of a distillation column in ProsDS basically consists of several flash separators combined together. In addition, some heat-exchangers can possibly be included. [6]

The distillation model utilized in the operator training simulators is currently restricting the development of operator training. The model does not take into account the capacity limits of the column. Hence, the model is not realistic and operators cannot be trained to operate the column in its limit conditions. The inner phenomena of a distillation column are not modelled in the current distillation model. As the column internals are not modelled accurately, it is not possible to examine the internal flows of the column. Training of inner phenomena of the column, like flooding, requires a more accurate distillation model that will also take tray hydraulics into consideration.

1.2 Distillation in other dynamic process simulators

There are several dynamic process simulators commercially available, which can be utilized in dynamic simulation of a distillation column. In process simulators, there usually is a graphical user environment that pictures the simulated model. Most process simulators can be divided into *sequential modular* or *equation-oriented* approaches. In sequential modular i.e. block-oriented approaches, every process consists of standardized blocks that model the behavior of a process unit or a part of it. Blocks are linked by connections that represent information, material or energy flow. The blocks are selected from the library, and the model built upon equations and variables, is hidden from the user. [7] A modular strategy is based on the concept that the solution of the individual units of the flowsheet is delegated into the unit level. This means that each unit operation is solved by means of an appropriate solver. Thus, the units provide only input-output information. Convergence is achieved by means of a certain coordination algorithm on the flowsheet level which is usually iterative. The dynamic sequential modular

simulation algorithm operates on bounded integration intervals. The integration continues until the end of the simulation time horizon is reached. [8] Sequential modular approach is user-friendly as it makes simulators easy to implement and understand, but the rigid blocks make it inflexible since the user cannot make any changes to the blocks. In equation-oriented approaches, modelling is addressed on the equations level and each block is solved independently. In addition, in equation-oriented simulators, a library of unit operations is available, but blocks can be modified as well. Although equation-oriented approach is more flexible than sequential modular, it can be demanding to use. [7] Some of the most established commercial dynamic process simulators are discussed below.

Aspen Plus Dynamics is a software program of Aspen Technology planned for dynamic process simulation. It is an extension to Aspen Plus and steady-state models from Aspen Plus can be imported to Aspen Plus Dynamics. Library of equipment models include rigorous distillation with hydraulics. In addition, Aspen Custom Modeler can be used for creating user-defined unit operations. [9]

The other dynamic simulation software solution of Aspen Technology is Aspen HYSYS Dynamics. It is integrated into Aspen HYSYS making the converting of steady-state process model into a dynamic process simulation model possible. Aspen HYSYS Dynamics focus mainly on time-dependent oil and gas processes, including gas processing and petroleum refining. [10] In Aspen HYSYS Dynamics, some coefficients considering hydraulic phenomena of the distillation column, as foaming factor, weeping factor and maximum flooding percent, can be specified in *Tray section*. [11]

Chemstation's CHEMCAD is a flexible chemical process simulation environment. It is capable of modelling batch, semi-batch and continuous systems. One of the CHEMCAD modules, CC-DYNAMICS, enables designing and rating processes using a dynamic simulation. Columns in CHEMCAD can be modelled as high- or low-fidelity. Distillation column can be chosen as tray or packed type. CHEMCAD also provides hydraulic performance such as predicted amount of flooding. [12]

Process Systems Enterprise's (PSE) process simulator gPROMS is an equation-oriented modelling and optimization software program. In gPROMS both steady-state and dynamic simulation can be done within the same framework. By using the gRPOMS language, it is also possible to create custom process models as the physical and chemical relationships representing the modelled process can be written down. [13] Utilizing this feature, nonlinear equations capturing the fluid behavior in the column can also be included in the model. Chang et al. [14] studied rigorous industrial dynamic simulation of a crude distillation column. In addition to material and energy balance and equilibrium relations, tray hydraulics was modelled with gPROMS.

The commercial process simulators always require licenses. Software packages that convert steady-state simulation to dynamic mode, especially if additional software is also needed for custom models, will often take more than one license reservation from the total number of licenses in the company. Thus in-house software has the benefit of free usage, even though the development of the software will require effort. Tu & Rinard [7] claim that although there are commercially available dynamic simulators, hardly any of them have a library of equipment that is extensive enough to satisfy even the needs of the most routine projects. Hence, the most important advantage of in-house software is the possibility to customize it according to the needs of the company.

1.3 Aim of this thesis

The aim of this thesis is to improve distillation modelling in ProsDS. In ProsDS the advantages of sequential modular and equation-oriented simulators come together since as a sequential modular simulator it is easy to use, but it is also flexible, because as in-house software, models can be modified when needed.

As described in the first subchapter, tray hydraulics is not taken into consideration in the current distillation model of the operator training simulators. Thus, operators cannot be trained to operate the column in its limit conditions and it is not possible to examine the internal flows of the column. In Neste, training and competence of the operators are highly valued. One part of the operator training system is the understanding of the inner phenomena in a distillation column. Currently, as the simulators cannot be utilized in this training due to the insufficient distillation model, there is educational material provided for the operators. However, it is noted that in addition to theoretical training, practical training with simulators is beneficial in understanding of the function of the processes. Training with simulators helps operators to understand how changes in processes affect the system dynamics.

In this thesis, the distillation model is improved, so that the model also considers tray hydraulics. The purpose of this is that the distillation model is able to take into account the vapor and liquid flow rate limits and model the consequences of exceeding these limits. The modelling is first outlined manually. The correlations for hydraulic phenomena are defined by utilizing KG-TOWER software of Koch-Glitsch. The tray and packing manufacturer Koch-Glitsch is a major company of designing and manufacturing mass transfer, mist elimination and liquid-liquid coalescing equipment in the field of refining, chemical, petrochemical and gas processing industries. After the correlations are defined, they are implemented in ProsDS by programming in ANSI Common Lisp.

As the distillation model is improved, it can be utilized in the operator training simulators. With the distillation model of a realistic behavior, the operators can be trained to recognize when a distillation column is approaching or exceeding the hydraulic constraints and thus operators can avoid upset situations and operate process faster back to

the normal condition. The model will also offer beneficial support for operator training considering the inner phenomena of a distillation column and provide a possibility to examine the internal flows of the column.

1.4 Content of thesis

The literature part of this thesis consists of Chapter 2 and Chapter 3. In the second chapter, tray and packed columns and hydraulic constraints of a tray column are discussed. In third chapter, basic equations and modelling of hydraulic constraints are presented.

The applied part of this thesis includes Chapters 4, 5 and 6. The current distillation model in a dynamic process simulator, KG-TOWER software as well as the defining of the correlation are described in Chapter 4. In Chapter 5 the development and implementation of the improved distillation model is represented. Chapter 6 consists of a discussion of the results as well as their sensibility and reliability. In addition, the future aspects are considered. Finally, the thesis is summarized in Chapter 7.

2. HYDRAULICS IN DISTILLATION COLUMN

The purpose of the column internals is to ensure separation of multicomponent mixtures by promoting an intimate contact of liquid and vapor. There are two types of distillation columns. One uses stages, i.e. trays or plates, to obtain a contact between the countercurrent flows of vapor and liquid. These are called tray columns. The second type of columns, packed columns, bring a differential contact between the countercurrent flows of vapor and liquid over the surface of some packing. [1, pp. 219−221]

In both types of columns, there are limits of operability near or beyond which the column will fail to function. These hydraulic constraints are critical and important to recognize. [1, p. 221] In the following chapter, first tray and then packed columns are elaborated. After that the hydraulic constraints of tray column operability are explored.

2.1 Tray columns

Many industrial distillation columns are equipped with trays or plates. Typically, these trays are equally spaced inside the cylindrical column shell. In each tray there are usually two conduits, one on each side, called downcomers. In addition to these one-pass trays, two-pass, three-pass and four-pass trays are also used to avoid excessively short liquid paths. Nevertheless, the number of passes should be minimized, since trays containing a large number of passes are prone to maldistribution. [15, p. 167] Due to gravity, liquid flows down from the tray through a downcomer, across the tray below and then over a weir into another downcomer. The weir on one side of the tray maintains the level of liquid on the tray at a desired level. The area between the downcomers is called the active area, where ascending vapor from the tray below passes through the liquid and makes contact with it. [1, pp. 4−5; 16, p. 2] A downcomer must be sufficiently large to permit the froth clarification to liquid and liquid to flow to the tray below without choking [15, p. 175]. The distance between two trays is called tray spacing. There is a vapor space above the active area. In that area, liquid is separated from vapor, as vapor flows up and sloshing liquid drops fall back to the active area. Prime factor in setting tray spacing is the economic trade-off between column height and column diameter. [17] In Figure 2.1 there is a schematic of a typical sieve type tray.

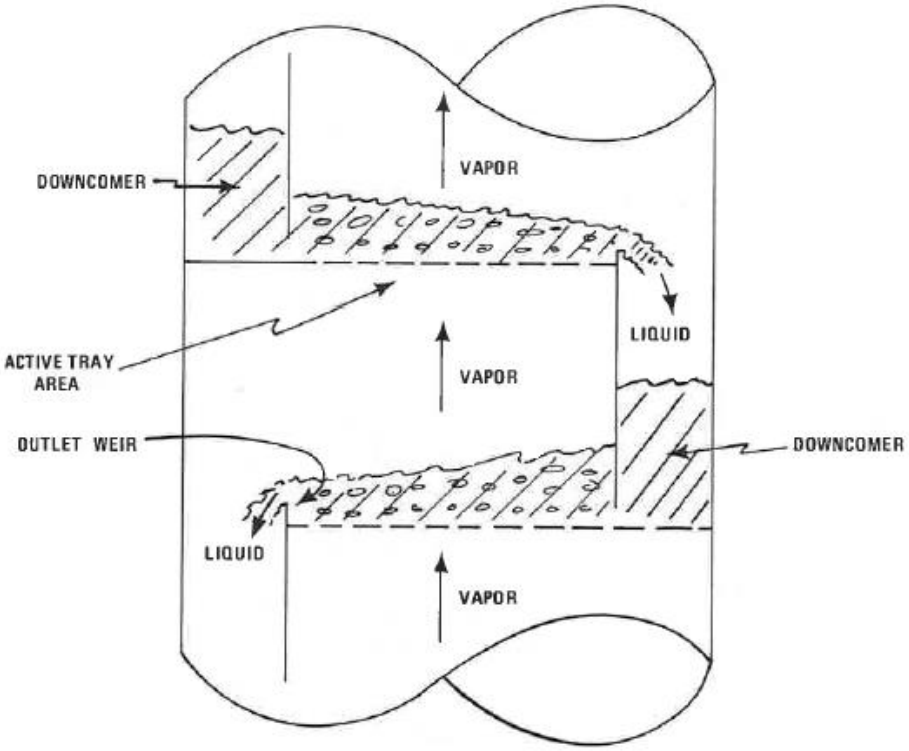

Figure 2.1. *Schematic of a typical sieve tray [4, p. 29].*

There are a variety of tray types available commercially. The simplest one is a sieve tray, which is a flat plate with a number of perforations that are provided for vapor flow. Vapor flow through the holes must be sufficiently high to prevent the liquid from falling through the holes. In Figure 2.2, the function of the sieve type tray is represented.

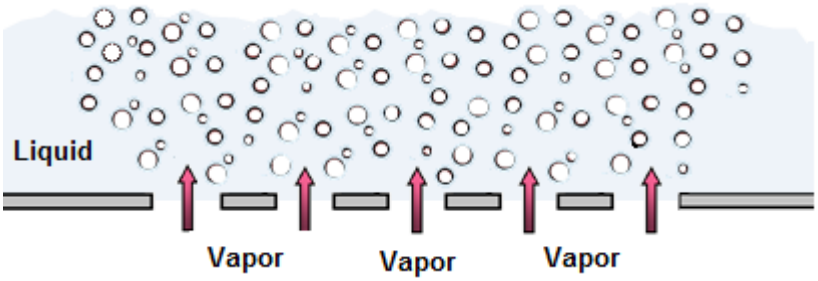

Figure 2.2. *Function of a sieve type tray. Adapted from [18].*

In a bubble-cap tray there is a riser or a chimney fitted over each hole and a cap covering the riser. The cap is mounted so that there is sufficient space between the riser and the cap for vapor to pass. Vapor rises through the chimney and is directed downward by the cap. Vapor discharges from the slots in the cap and bubbles through the liquid on the tray. Figure 2.3 shows the basic function of a bubble-cap tray. The components of a bubble-cap are also presented in the figure.

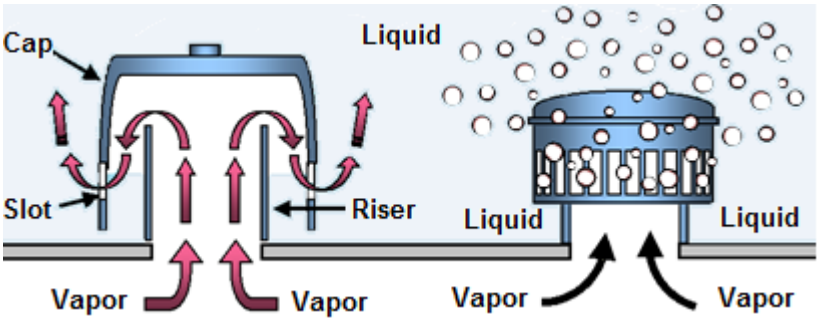

Figure 2.3. *Function of a bubble-cap tray. Adapted from [18].*

Bubble-cap trays were the best-known vapor-liquid contacting devices in chemical industry for years, but valve trays have since become more common in distillation operations. In a valve tray, the perforations are covered with caps that can be lifted. Upward flowing vapor lifts the cap, thus creating a flow area for the vapor passage. Vapor flows horizontally into the liquid, and therefore a better mixing is provided than in sieve trays where the vapor passes straight upward through the liquid. Sieve and valve trays have replaced bubble-cap trays in many applications due to their high efficiency, wide operating range and low cost. [1, pp. 4−5] In Figure 2.4 the function of a valve tray is illustrated with normal, low and high vapor flow.

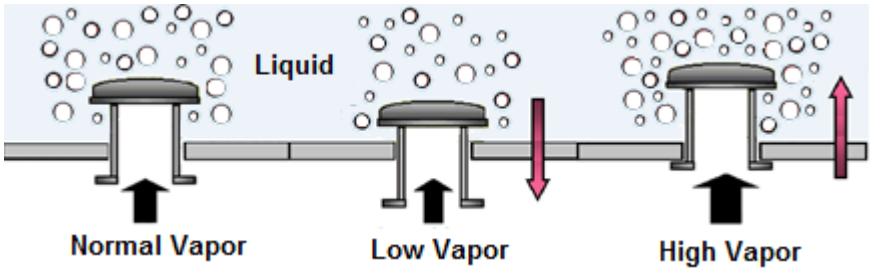

Figure 2.4. *Function of a valve tray. Adapted from [18].*

Trays in a distillation column promote mass transfer of heavy components into the liquid flowing down the column and of light components into the vapor flowing up the column. Vapor flows from one tray up to another through the tray above, because the pressure is lower on the upper tray. Thus there is an increase on pressure from the top of the column to its base. Liquid phase is denser than the vapor phase. Hence, the liquid flows against the positive pressure gradient. In the downcomer, liquid level is built up to a height sufficient to overcome the static pressure difference between two trays. The pressure difference depends on the vapor pressure drop through the tray and the average liquid height on the tray. [4, pp. 28−29] In order for liquid to flow through the downcomer to the tray below and to prevent vapor to flow flowing through the downcomer, the hydrostatic pressure of the liquid in the downcomer must compensate the liquid flow resistances in the downcomer and in transfer to the active area, in addition to the pressure loss of the tray [19].

2.2 Packed columns

While trays are evenly spaced apart, packing usually fills all of the available space inside a column. All the various packings are based on the fact that an effective mass transfer between liquid and vapor requires an extensive surface. For good separation, the liquid and vapor should be uniformly spread over the cross-section of the column. Redistribution and intermixing should be frequent with the film thickness remaining as uniform as possible. The packing elements should be low-weight and mechanically and chemically resistant. In addition, the pressure loss of the vapor flowing through the packing should be small. As none of the known packings offers a maximum of all these, it must be decided, which type of packing is the most suitable in each case. In all types of packings the separation effect depends significantly on a uniform distribution of the reflux across the column cross-section. [20, p. 86] In the past several decades, following the appearance on the market of high-performance packings, continuous vapor-liquid devices have replaced trays with respect to increasing column capacity and/or reducing pressure drops [1, pp. 21−22]

In packed columns, the liquid-vapor contacting is achieved with packed beds i.e. packings. Liquid and vapor flow in the counterflow direction and zigzag through the column. Even relatively small reflux quantities will be uniformly dispersed into the liquid film, because of the strong capillary action of the surfaces. The inclination of the channels formed provides good intermixing of the phases. [20, p. 92] Two types of packings can be used in the distillation column: a random packing or a structured packing. Random packings usually consist of 1-3 cm sized pieces. The pieces of random packings are usually either some kind of rings or saddles. The structured packings are systematically shaped for achieving a good vapor-liquid contact. [19]

As the problems of the packed columns are usually uniform liquid distribution and maintaining the distribution, there are several devices for distribution in a packed column [19]. The main devices for setting the quality of distribution are the top or reflux distributor, the intermediate feed distributor, the redistributor and sometimes the vapor distributor [15, p. 35]. Beside packings and distributors, the packed column internals also include packing supports that physically support the packed bed while permitting unrestricted flow of liquid and vapor [15, p. 211]. In Figure 2.5 typical internals of a packed column are represented.

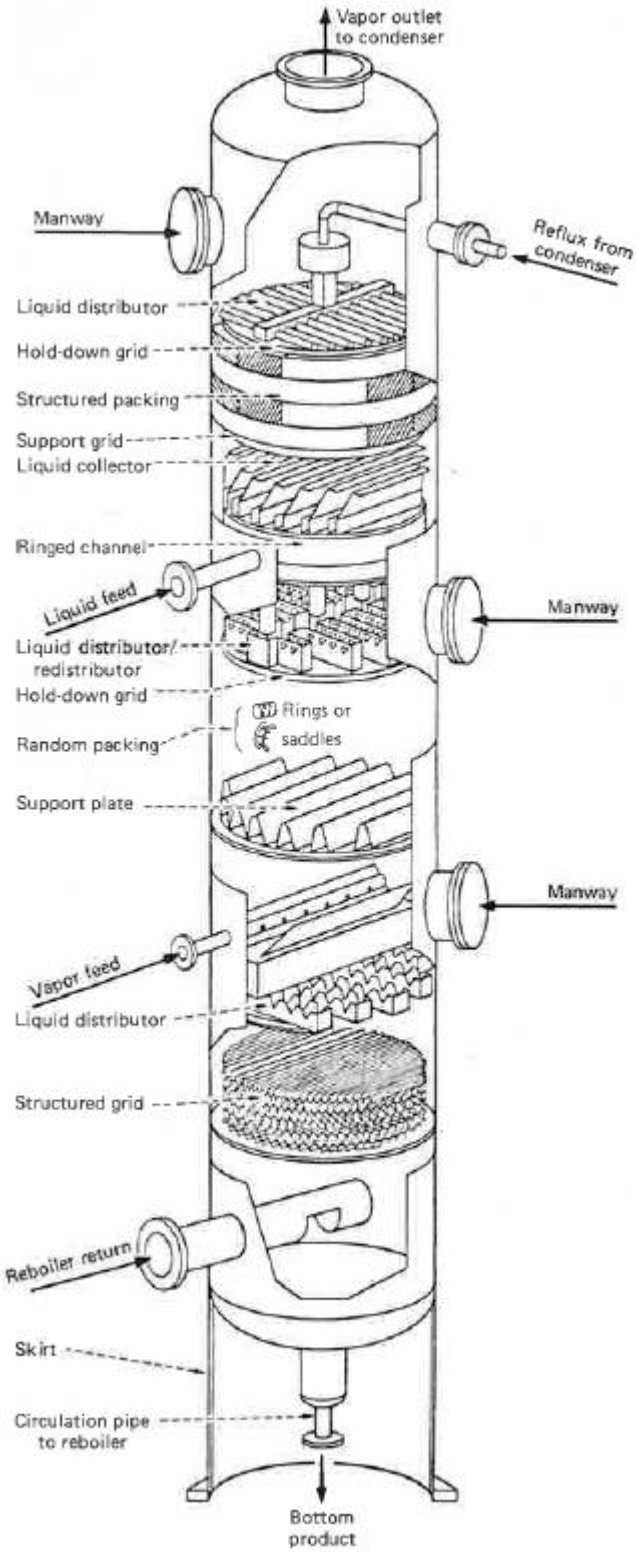

Figure 2.5. *A cutaway of a packed column [15, p. 212].*

The capacity of a packed column is usually restricted by vapor flow. Great vapor flow rate will increase the pressure loss and sometimes also decrease the column efficiency.

2.3 Hydraulic constraints

Column throughput is restricted by one of several different mechanisms [15, p. 141]. These mechanisms are outlined in this subchapter. The efficient and safe operation zone of a distillation column is bounded by vapor and liquid flow rates. In Figure 2.6 the effect of vapor and liquid flow rates on operation is presented.

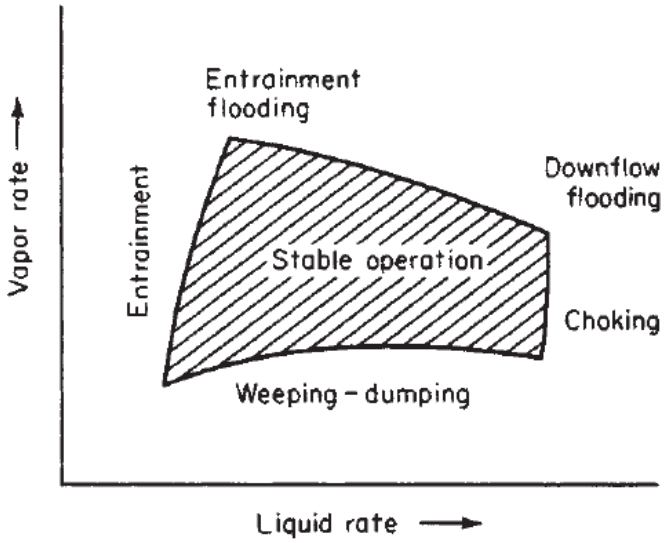

Figure 2.6. *Stable operating zone for tray columns [21].*

Flooding in a distillation column is excessive accumulation of liquid on a tray [15, p. 376]. Flooding is synonymous with the distillation column maximum capacity and reaching this limit is detected by a sharp increase in the pressure drop. There are two types of flooding mechanisms, jet flooding and downcomer flooding. Weeping is a phenomenon that can occur especially in perforated tray columns while foaming is an expansion of aerated liquid. [1, pp. 221−222]

2.3.1 Jet flooding

Jet flooding is triggered by excessive liquid entrainment [1, p. 134]. Entrainment occurs if vapor flow rate and velocity are too high considering liquid flow rate and tray cross-section area [19]. Entrainment is defined as liquid drops carried away with vapor from the tray to the one above [1, p. 221]. It is detrimental for two reasons. Since liquid of lower volatility is carried to the tray containing liquid of higher volatility, entrainment lowers the tray efficiency. It can also contaminate the high-purity distillate, since it carries nonvolatile components upwards. Thus, there is a maximum value for vapor flow velocity between trays that cannot be exceeded. [19] In Figure 2.7 the condition of jet flooding compared to the normal operation of a distillation column is illustrated.

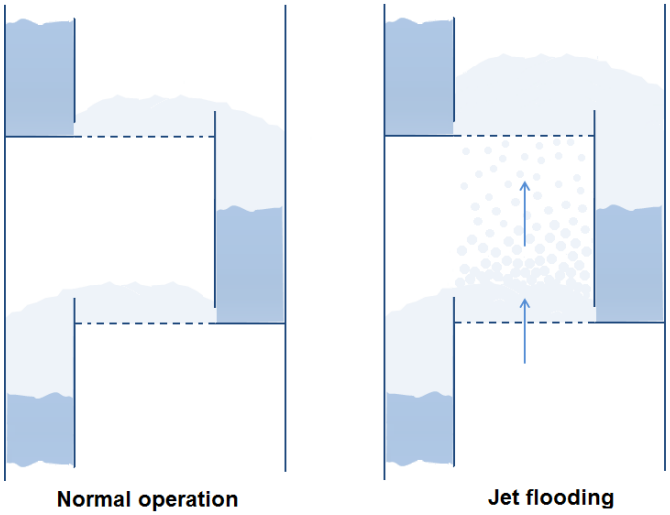

Figure 2.7. *Jet flooding.*

When jet flooding begins, the downcomer can be only partially filled with liquid. As jet flooding develops further, the downcomer becomes filled with liquid and all of the liquid fed to the tray is carried to the tray above. Jet flooding is characterized by a large increase in the pressure drop across the column as the column becomes flooded. [16, p. 424]

There are two mechanisms identified for entrained drop generation. The mechanism depends on the flow regime. Different correlations are required in the spray and froth regimes. In the spray regime, entrainment increases with increased vapor velocity in tray holes and diameter of the holes. Entrainment decreases with increased liquid weir load and fractional perforated area. In the froth regime, entrainment primarily depends on the approach of the upper surface of the froth to the tray above. The factors that increase froth height, increase entrainment. Those factors are vapor velocity, liquid load and weir height. In both regimes, a reduction of tray spacing increases entrainment. [22, pp. 94−95]

2.3.2 Downcomer flooding

Downcomer flooding occurs when the liquid height in the downcomer equals or exceeds the height between trays i.e. tray spacing [4, p. 30]. Flooding is caused by too high liquid flow rate. If downcomer flooding occurs, a sharp increase in pressure drop across the column is observed. [16, p. 424] Downcomer flooding is caused either by downcomer backup flooding mechanism or downcomer choke flooding mechanism.

Liquid is conveyed through the downcomer from a lower to a higher pressure. Consequently, liquid backs up in the downcomer to overcome the pressure difference. Thus, it is essential that downcomer height is sufficient to accommodate this backup to avoid flooding. [22, pp. 98−99] However, when liquid flow is raised, pressure drop of the tray

along with liquid height on the tray and frictional losses in the downcomer increase. Consequently, aerated liquid on the tray is backed up to the downcomer. When the backup of aerated liquid in the downcomer exceeds the tray spacing, liquid accumulates on the tray above. This phenomenon is called downcomer backup flooding. [15, p. 376]

Downcomer must be sufficiently large to transport all liquid downflow. Downcomer choke flooding occurs as the velocity of aerated liquid in the downcomer increases due to the liquid flow rate increase. When the velocity of aerated liquid exceeds a certain limit, friction losses in the downcomer and its entrance become excessive. Consequently, all of the frothy mixture cannot be transported to the tray below, which causes accumulation of the liquid on the tray above. [15, pp. 376−377] In addition, excessive flow rate of vapor venting from downcomer in counterflow, will impede liquid downflow [21]. In Figure 2.8 downcomer flooding mechanism of both downcomer backup and downcomer choke are presented beside the normal operation of a tray column.

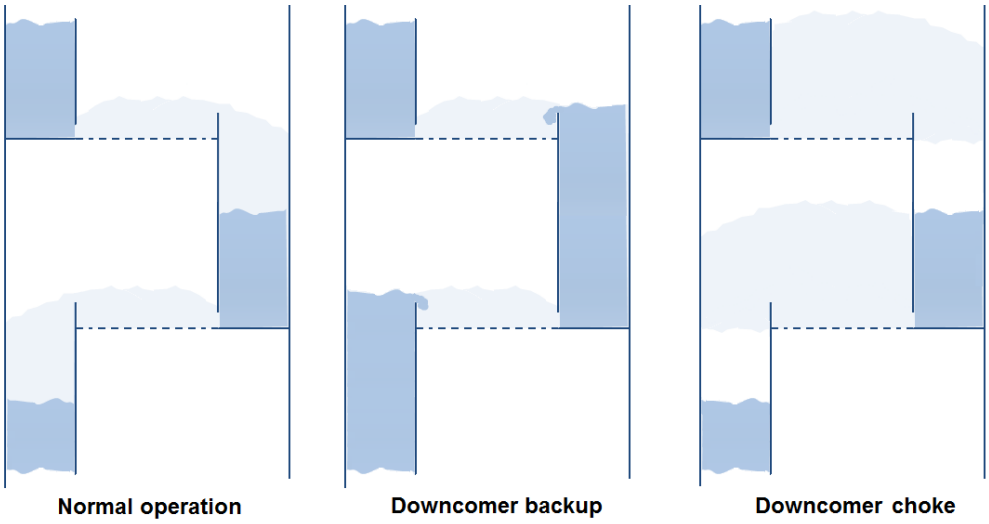

Figure 2.8. *Downcomer flooding caused by downcomer backup and downcomer choke.*

Downcomer choke flooding is also called downcomer entrance flooding or downcomer velocity flooding. The prime parameter in downcomer design that affects the downcomer choke flooding is the downcomer top area. Further down the downcomer, vapor disengages from liquid, and thus the volumes of aerated liquid flowing down and vented vapor flowing up are greatly reduced. [21]

2.3.3 Weeping

In perforated tray columns, if vapor rates are decreased, a point is reached at which the liquid head on the tray is equal to the pressure holding it on the tray. Consequently the vapor pressure drop through the openings in the tray is not high enough to keep liquid from flowing down through the perforations. This is known as weeping. Weeping occurs to some extent over a range of conditions due to sloshing and oscillation of the liq-

uid on the tray, but when it becomes continuous and excessive, the phenomenon is called dumping. In that case, all the liquid fed to the tray weeps through the holes of tray and no liquid flows over the weir to the downcomer. Dumping affects seriously the operation of the column and leads to a sharp decrease in efficiency and increase in pressure drop [1, p. 222] If weeping occurs, fractionation suffers as vapor-liquid contacting is poor [4, p. 30]. Figure 2.9 illustrates weeping in a distillation column.

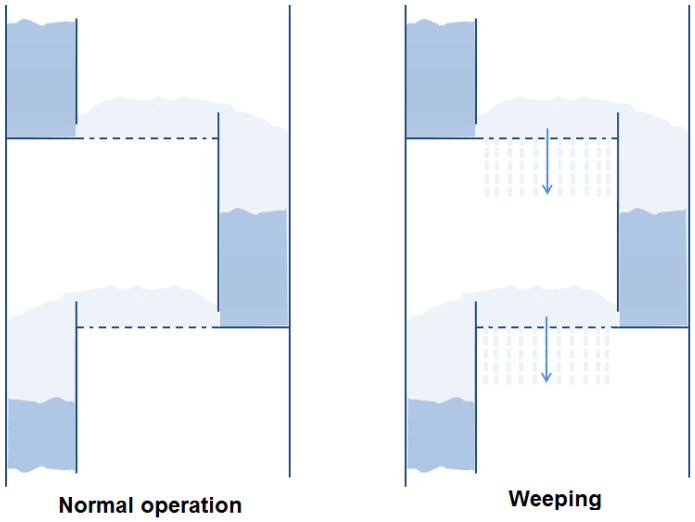

Figure 2.9. *Weeping occurring in a sieve type tray.*

The main factor affecting weeping is the fractional hole area. The larger the area is, the smaller the vapor pressure drop and consequently, the greater the weeping tendency. Larger liquid rates and higher outlet weirs also increase the liquid heads on the tray and therefore weeping as well. Weeping is often non-uniform. Some hydraulic conditions favor weeping from the tray inlet and others from the tray outlet. Weeping from the tray inlet is particularly detrimental to tray efficiency as the weeping liquid bypasses two trays. [21]

Valve trays can be operated at relatively low vapor rate because the valve openings close as the vapor rate decreases. Bubble-cap trays can operate at very low vapor rate due to their sealing arrangement. Thus, weeping does not occur in distillation columns of bubble-cap trays. [16, p. 424]

2.3.4 Foaming

Foam forms when vapor bubbles rise to the liquid surface and persist without coalescence with one another or without rupture into the vapor space [15, p. 393]. Since foaming provides a high interfacial area for the vapor-liquid contact, it is desirable to a certain degree. However, excessive foaming results in a liquid buildup on the tray. If the foam buildup becomes high enough to pass through the risers in a bubble-cap column or through the holes in a perforated-tray column to mix with the liquid on the tray above,

the condition is known as priming. That greatly reduces the separation efficiency of the column. [1, p. 221] In Figure 2.10 foaming in a distillation column is illustrated.

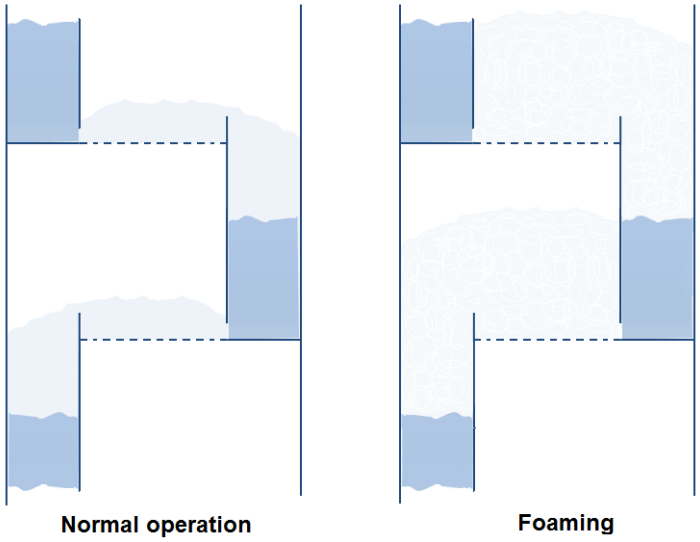

Figure 2.10. *Foaming in a distillation column.*

Foaming is primarily a function of the physical properties of the liquid. In addition, the method and degree of aeration impact foaming. [1, p. 221] Foaming can be prevented with foam inhibitors. They are insoluble materials and spread spontaneously over the surface of the foamy liquid. The film of foamy liquid is replaced by a film of spreading liquid, which cannot support an extended liquid film, thus causing rupture. [15, pp. 396−397] The disadvantages of foam inhibitors are their cost and the possibility of product contamination [22, p. 53].

3. MODELLING OF HYDRAULICS

The mathematical model formed for a process describes the system behavior on equation level. It introduces the most essential factors concerning the process and causal relationships between process variables. Highly accurate models are extremely complicated and both forming and solving them take plenty of time. Depending on the application, some assumptions can be made about the process behavior, so that the model will be simpler. It is essential to derive the simplest possible model that is capable of a realistic representation of the process. [23, pp. 1−3]

Forming the mathematical model for a distillation column is based on fundamental conservation laws of mass and energy. By means of these conservation laws the mass, component and energy balances can be formed. In addition, there are algebraic equations involved. They describe hydraulics in the column and also physical properties of the components. In this chapter, the basic equations and modelling of hydraulic phenomena are presented.

3.1 Basic equations

Tray columns are usually modelled by using balance equations. The mass, energy and component balances are presented in this subchapter. After that, vapor-liquid equilibrium (VLE) and tray efficiency are considered. Each additional component of the feed mixture must be expressed by a separate component material balance and by its own equilibrium relationship. The pressure drop of a tray is also examined in this subchapter.

3.1.1 Balance equations

The basic principle for modelling conservation of mass or matter can be expressed as

$$Accumulation = In - Out. \tag{1}$$

That is to say, the rate fed into the system must equal the rate that comes out or accumulates in the system [23, pp. 4−10]. The system in this content can be a tray in a distillation column. In a steady-state system there is no accumulation, but in a dynamic process model accumulation usually occurs. The equation (1) is valid for mass and energy balances and can be applied for each chemical component of the system, provided no chemical change occurs. In component balance, the change due to reaction can be taken into account by adding a reaction term into the equation (1).

In Figure 3.1 a tray *i* of a distillation column is presented. The tray is heated with a heat supply Q_i and the feed F_i to the tray can be either vapor or liquid or a mixture of both. In addition, a vapor product flow PV_i or liquid product flow PL_i can be taken out of the tray. If some of these do not exist, they can be set to value 0 in the model. The vapor flow V_{i+1} comes to the tray *i* from the tray below and the vapor flow V_i goes to the tray above. On the contrary, the liquid flow L_{i-1} comes to the tray *i* from the tray above and the liquid flow L_i goes to the tray below.

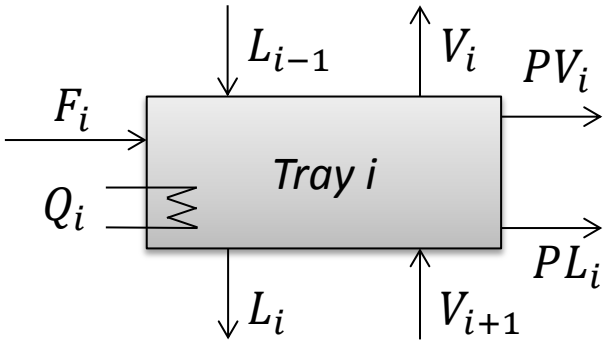

Figure 3.1. *A scheme of a separation state of the tray i. Adapted from [24].*

For each tray, the mass and energy balances can be formed. In addition, *n-1* component balances can be formed for *n* components in a tray *i*. The balances are in form of differential equations. [24]

The total mass balance for two phases can be presented as

$$\frac{d(M_i)}{dt} = F_i + L_{i-1} + V_{i+1} - L_i - V_i - PL_i - PV_i \,, \tag{2}$$

where the total molar holdup M_i in the tray *i* is the sum of the molar liquid holdup and the molar vapor holdup in the tray *i*, that is $M_i = M_i^L + M_i^V$. When two phases come into contact, there is a net flow of material from one phase to another until equilibrium is reached. In steady-state situation the value of the equation (2) is 0.

The mass balance of a component between two phases can be expressed as

$$\frac{d(M_{i,n})}{dt} = F_i x_{F,n} + L_{i-1} x_{i-1,n} + V_{i+1} y_{i+1,n} - L_i x_{i,n} - V_i y_{i,n} - PL_i x_{i,n} - PV_i y_{i,n} \,, \tag{3}$$

where the molar holdup of the component *n* in the tray *i* can be presented as $M_{i,n} = M_i^L x_{i,n} + M_i^V y_{i,n}$. In the equation (3) $x_{F,n}$ is the mole fraction of the component *n* in the feed, $x_{i-1,n}$ is the mole fraction of the component *n* in liquid phase coming to the tray *i*, $x_{i,n}$ is the mole fraction of the component *n* in liquid phase leaving the tray *i*, $y_{i+1,n}$ is the mole fraction of the component *n* in vapor phase coming to the tray *i* and $y_{i,n}$ is the mole fraction of the component *n* in vapor phase leaving the tray *i*.

The energy balance and the mass balance of a system interrelate with each other. The internal energy depends on temperature, mass and composition of the system. [23, p. 22] The energy balance can be written as

$$\frac{d(M_i h_i)}{dt} = F_i h_i + L_{i-1} h_{i-1} + V_{i+1} H_{i+1} - L_i h_i - V_i H_i - PL_i h_i - PV_i H_i - Q_i. \quad (4)$$

In the equation above, $M_i h_i$ is the molar holdup of the liquid phase enthalpy in the tray *i*, h_F is the enthalpy of the feed, h_{i-1} is the enthalpy of the liquid phase coming to the tray *i*, h_i is the enthalpy of the liquid phase leaving the tray *i*, H_{i+1} is the enthalpy of the vapor phase coming to the tray *i* and H_i, is the enthalpy of the vapor phase leaving the tray *i*.

3.1.2 Equilibrium relations

The system state equilibrium can be determined with the help of an equilibrium constant. The equilibrium between vapor and liquid phases is determined as

$$y_{i,n} = K_{i,n} x_{i,n} \, , \quad (5)$$

where $K_{i,n}$ is the equilibrium constant for the component *n* in the tray *i*. The sum of the mole fractions in liquid phase in the tray *i* equals the sum of the mole fraction in vapor phase in the tray *i* and is valued as 1. With the equation (5), the vapor phase composition can be calculated if the composition of liquid is known and vice versa. In an ideal mixture, Raoult's and Dalton's laws can be used for determine the *K* values:

$$K_{i,n} = \frac{y_{i,n}}{x_{i,n}} = \frac{P_{i,n}^0}{P_i}. \quad (6)$$

In the equation (6) $P_{i,n}^0$ is the vapor pressure of component *n* in pure liquid phase in the tray *i* and P_i is the total pressure in the tray *i*. However, many mixtures show non-ideal behavior in the liquid phase. In such cases, the equation (6) is modified to include the liquid activity coefficient $\gamma_{i,n}$. At high pressure conditions, the vapor fugacity coefficients ϕ_n become necessary for the better equilibrium defining. In this condition the equation is

$$K_{i,n} = \frac{P_{i,n}^0 \gamma_{i,n}}{P_i \phi_n} \, . \quad (7)$$

The liquid activity coefficient $\gamma_{i,n}$ depends on the composition of the liquid phase. The standard state of reference is $\gamma_{i,n} = 1$ for a pure component *n*. [3, pp. 3−4]

In distillation, the separation is based on the different composition between vapor and liquid in equilibrium. In ideal equilibrium stage, one or more material or energy streams enter and one vapor and one liquid stream leave the stage in thermodynamic equilibrium. [3, p. 8] Real trays in a distillation column are not ideal and do not function as ideal

stages. Vapor leaving the tray is not in equilibrium as determined in the equation (5), if the contact time between vapor and liquid is too short. The high viscosity derives small diffusion coefficients and poor mass transfer, resulting in low efficiency. In addition, high pressure often deteriorates the function of the trays and packings. [19] A commonly adopted approach to evaluate the operation of a real tray is to add to the model Murphree tray vapor efficiency, which is defined as

$$E_{i,n} = \frac{y_{i,n} - y_{i+1,n}}{y^*_{i,n} - y_{i+1,n}}. \quad (8)$$

In the equation (8), the vapor mole fraction of the component *n* leaving the tray *i* in equilibrium is defined as $y^*_{i,n} = K_{i,n}x_{i,n}$. Murphree vapor efficiency is thus the ratio of the vapor mole fraction change across the tray to the change that would occur across an ideal stage for a specific component *n*. If there are *m* components in the vapor phase, *m-1* Murphree vapor efficiencies could be defined. [3, p. 20]

As in ProsDS the distillation column is modelled by combining flash tanks, the vapor-liquid equilibrium (VLE) is calculated in the blocks and do not require any further consideration. The more rigorous examination of vapor-liquid equilibrium can be found in the literature of the field, for example Distillation Tray Fundamentals [22] and Fundamentals of Multicomponent Distillation [16].

3.1.3 Pressure drop

The pressure drop over the downcomer from the surface of the liquid exiting the downcomer to the surface of the downcomer level equals the total pressure drop over a tray. The flow under the downcomer apron is modelled by instationary Bernoulli equation. In the equation (9), the pressure loss due to friction and the acceleration of the liquid under the downcomer apron have been taken into consideration. The pressure drop over the tray can be defined as

$$\Delta p_{tray} = \rho_L g h_{dc} - \zeta v_{dc}^2 \rho_L - L\rho_L \frac{v_{dc}}{dt}, \quad (9)$$

where the velocity under the downcomer apron is

$$v_{dc} = \frac{Q_t}{A_{apron}}. \quad (10)$$

The characteristic length L is chosen to be equal to the height of the downcomer apron. In the equation (9) ρ_L is the liquid mass density, g is the standard acceleration of gravity, h_{dc} is the liquid height in the downcomer and ζ is the resistance coefficient. In the equation (10) Q_t is the liquid flow under the downcomer and A_{apron} is the area of downcomer apron. [25]

The total pressure drop over a tray is the difference of the pressure of the vapor entering and the vapor leaving the tray. The total pressure drop over a tray equals the sum of the liquid head on the tray Δp_{static} and the dry pressure drop Δp_{dry} and the residual pressure drop Δp_r.

$$\Delta p_{tray} = \Delta p_{static} + \Delta p_{dry} + \Delta p_r \tag{11}$$

The pressure drop caused by clear liquid head on the tray active area is

$$\Delta p_{static} = \rho_L g h_{cl}, \tag{12}$$

where h_{cl} is the clear liquid height on the tray. The dry pressure drop is the pressure drop of the vapor flow through the perforated area without liquid flow. There are numerous correlations available for the dry pressure drop. The usual practice is to represent the dry pressure drop as

$$\Delta p_{dry} = \frac{1}{2}\xi \rho_V v_h^2 \, . \tag{13}$$

In this orifice-type equation, ξ is the orifice coefficient, ρ_V is the vapor density and v_h is the vapor velocity through holes in a tray. [22, pp. 76−77] The residual pressure drop should take into account several interacting dynamic phenomena between vapor flow and liquid. Usually, it can be considered constant, and in several cases it is negligible. [3, pp. 157−158]

3.2 Modelling of hydraulic phenomena

The modelling of hydraulic constraints is not simple and there are no straightforward physical equations for modelling hydraulic phenomena in a distillation column. Nonetheless, there are many different correlations concerning jet flooding, downcomer flooding and weeping available in the literature. In this subchapter, some correlations for hydraulic phenomena considered in this thesis are presented.

3.2.1 Modelling of jet flooding

The prediction of the onset of jet flooding using a fundamental approach is difficult, because correlations for liquid entrainment are insufficiently accurate. Thus, the approach taken is to utilize an empirical jet flooding correlation. There are some jet flooding correlations at least made by Fair [26] and Glitsch [27]. The capacity factor *CF* is defined as

$$CF = v_V \sqrt{\frac{\rho_V}{\rho_L - \rho_V}}, \tag{14}$$

where the superficial vapor velocity v_v is the ratio between the vapor flow rate Q_V and the active tray area A_a, this is

$$v_V = \frac{Q_V}{A_a} . \tag{15}$$

For commercial reasons, the jet flooding correlations are often formed differently in manufacturers' manuals. Glitsch correlation uses system factor *SF*, which lowers the capacity factor if the system is known to foam. [22, pp. 88−90] Thus, the capacity factor is expressed as

$$CF = CF_0 * SF . \tag{16}$$

where CF_0 is the capacity factor at zero liquid load. The values of the system factor *SF* have been given in Table 3.1. For non-foaming regular systems the system factor has a value 1.

Table 3.1. *System factors for different foaming systems. Adapted from [22, p. 52].*

	System factor SF
Slight foaming	0.90
Depropanisers	0.90
Freons	0.90
H_2S strippers	0.90
Hot carbonate strippers	0.90
Moderate foaming	0.85
De-ethanisers	0.85
Oil absorbers	0.85
Amine strippers	0.85
Glycol strippers	0.85
Sulpholane systems	0.85
Crude towers	0.85
Hot carbonate absorbers	0.85
Furfural refining	0.80
Heavy foaming	
Amine absorbers	0.75
Glycol contactors	0.65
Methylethyl ketone	0.60
Stable foam	
Alcohol synthesis absorbers	0.35
Caustic regenerators	0.30

The Glitsch correlation for jet flooding with different tray spacing for Ballast trays is presented in Figure 3.2. The figure shows that the capacity factor at zero liquid load is a function of vapor density and tray spacing.

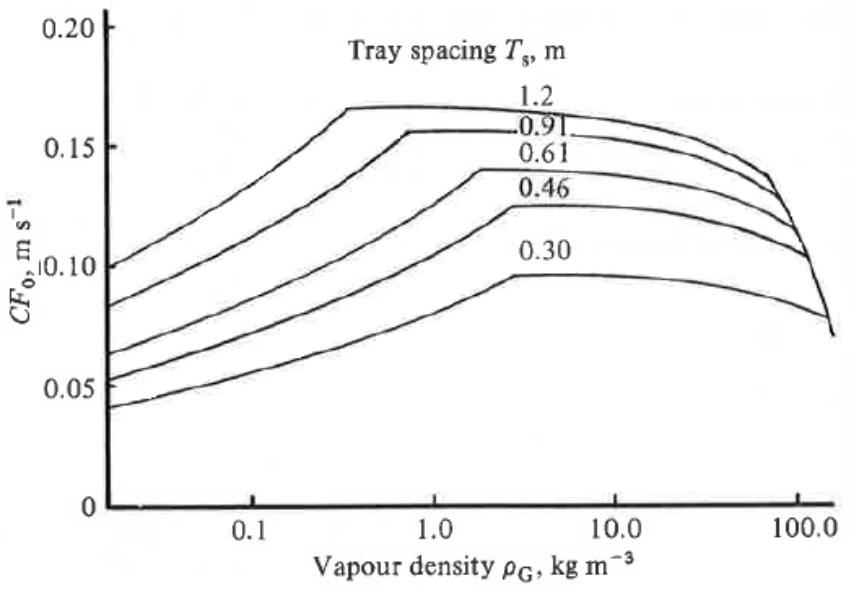

Figure 3.2. *The flooding correlation for Glitsch Ballast valve trays [26, p. 89].*

The capacity of Ballast trays increase with increasing tray spacing up to a limiting value. The energy dissipated by vapor flowing through a tray and the quantity of entrainment generated increase as the vapor density decreases. [27]

3.2.2 Modelling of downcomer flooding

As presented in the previous chapter, there are two different mechanisms for downcomer flooding. Downcomer backup h_{fd} is calculated from the pressure balance

$$h_{fd} = \frac{h_t + h_{cli} + h_{udc} - h_n}{\bar{\alpha}_d}, \tag{17}$$

where h_t is the total pressure drop across the tray, h_{cli} is the clear liquid height at the liquid entry, h_{udc} is the pressure drop for flow under the downcomer, h_n is the pressure increase across the nappe and $\bar{\alpha}_d$ is the mean liquid volume fraction in the downcomer [22, p. 99]. In Figure 3.3, the terms used in the equation (17) are illuminated.

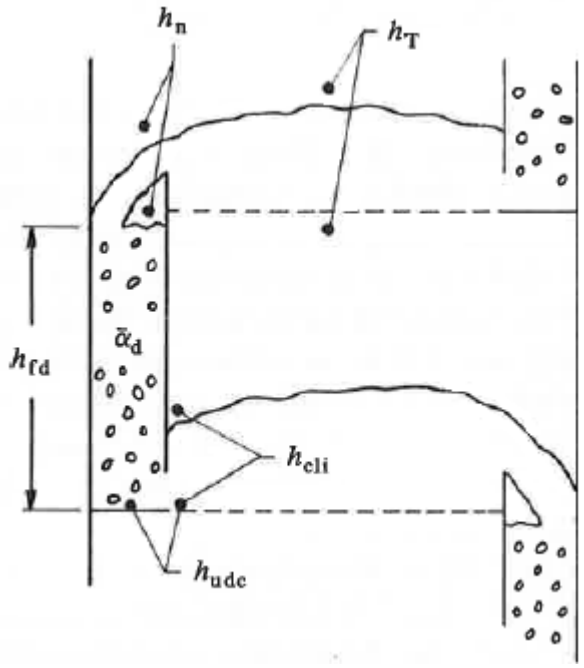

Figure 3.3. *Nomenclature for liquid backup in the downcomer [22, p. 99].*

At high pressure the equation (17) can be elaborated to also consider vapor density. Despite the simplicity of the equation (17), some of the terms are difficult to predict. The dominant term, the total pressure drop h_t, can be predicted with reasonable accuracy. The clear liquid height at liquid entry h_{cli} can be estimated various ways. The simplest assumption is to take it equal to the clear liquid height on the tray. It can be increased appropriately, if hydraulic gradient is significant. The pressure drop under the downcomer h_{udc} is given by

$$h_{udc} = \frac{1}{2g}\left(\frac{Q_L}{W h_1 C_d}\right)^2, \tag{18}$$

where Q_L is the liquid flow rate, W is the weir length, h_1 is the clearance under the downcomer and C_d is the discharge coefficient. The values of the discharge coefficient C_d used by tray manufacturers are *0.54* for Glitsch [27], *0.56* for Koch Engineering [28] and *0.60* for Nutter Engineering [29]. A pressure increase across the nappe h_n, is created when throw of froth over the weir acts as a seal at the mouth of the downcomer. It is significant for narrow downcomers and foaming systems, but almost always neglected in calculating downcomer backup since it is conservatively acting and reduces backup. [22, pp. 99−100]

For the other downcomer flooding mechanism, downcomer choke, there is no satisfactory published correlation. Nevertheless, a critical value for maximum velocity of clear liquid at the downcomer entrance exists. If the critical velocity is exceeded, choking occurs. Kister [15] has surveyed the multitude of published criteria for maximum downcomer velocity and incorporated them into single set of guidelines. [21] This is presented in Table 3.2.

Table 3.2. *Maximum downcomer velocities. Adapted from [21].*

Foaming tendency	Example	Clear liquid velocity in downcomer [m/s]		
		457 mm Tray spacing	610 mm Tray spacing	762 mm Tray spacing
Low	Low-pressure (< 7 bar) light hydrocarbons, stabilizers, air-water simulators	0.12−0.15	0.15−0.18	0.15−0.18
Medium	Oil systems, crude oil distillation, absorbers, mid-pressure (7 -21 bar) hydrocarbons	0.09−0.12	0.12−0.15	0.12−0.15
High	Amines, glycerin, glycols, high-pressure (>21 bar) light hydrocarbons	0.06−0.08	0.06−0.08	0.06−0.09

The values of Table 3.2 are not conservative. For conservative use, the values of Table 3.2 should be multiplied by a safety factor of *0.75*. For very highly foaming systems, where antifoam application is undesirable, the maximum velocity of *0.03−0.05 m/s* is beneficial. [21]

3.2.3 Modelling of weeping

Some weeping usually occurs in all conditions due to sloshing and oscillation of the tray liquid. Generally, as the weeping is small, it does not affect the tray efficiency. The weep point is the vapor velocity at which weeping becomes noticeable. As the vapor velocity is reduced below the weeping point the weep rate increases. [21] The weep rate typically varies with the vapor velocity. A higher exit weir increases the clear liquid height and consequently the weep rate is increased. [22, p. 108]

There are several approaches for theoretical prediction of the weep point. One theoretical approach according to Lockett [22] was adopted by Ruff et al. [30] who considered the stability of the vapor jet connecting a growing bubble to the hole. For ensuring that no weeping occurs, it was suggested that for small holes

$$\frac{\rho_V d_h v_h^2}{\sigma} > 2.0 \ (2.7 \ for \ safety) \tag{19}$$

and for large holes

$$\frac{v_h^2}{g d_h}\left(\frac{\rho_V}{\rho_L - \rho_V}\right)^{1.25} > 0.37 \ (0.75 \ for \ safety). \tag{20}$$

The transition between small and large holes is given by

$$d_h = 2.32\left(\frac{\sigma}{\rho_V g}\right)^{0.5}\left(\frac{\rho_V}{\rho_L - \rho_V}\right)^{0.625}. \tag{21}$$

In the equation (19) d_h is the hole diameter and σ is the surface tension. Except for cryogenic application, the holes used in sieve trays are usually determined as *large*. [22, pp. 110−112]

3.2.4 Modelling of foaming

Bubble coalescence proceeds by drainage of the intervening liquid film. Foam will tend to form when there is a mechanism that maintains the film and prevents it from rupturing prematurely during the drainage process. The stability of the foam depends on the foam's ability to heal itself against excessive localized thinning as overall film drainage proceeds. A range of foam types can be obtained depending on the degree of film stability. If film stability is only slight, unstable foam can barely be distinguished from froth. Metastable foams persist much longer and the bubbles become distorted into pentagonal dodecahedra to give what is usually called cellular foam. [22, pp. 44−45]

The extent of foaminess and its actual effect on distillation column capacity are difficult to predict from chemical composition and process conditions. However, the effect tends to be reproducible and is often lumped into a system factor. [31, p. 208]. The system factors for different foaming systems were presented in Table 3.1. As foaming is usually covered with a system factor, modelling of the foaming is not discussed in the literature of the field.

4. DISTILLATION MODELLING IN DYNAMIC SIMULATOR

There are no exact physical equations for modelling the hydraulic phenomena in a distillation column. The correlations presented in Chapter 3 are not straightforward and contain parameters that are difficult to determine. Therefore in this thesis, it is decided to utilize tray and packing manufacturer's software to determine the required correlations between vapor and liquid flows and the tray hydraulics. Thus, the manufacturer is also responsible of the knowhow development. Nevertheless, as a disadvantage, the use of the manufacturer's software derives a reliance of the software. In addition, the software's correlations for high performance trays are insufficient and the manufacturer needs to be consulted.

In this chapter, the current distillation model in ProsDS is explored in more detail. In addition, the manufacturer's software, KG-TOWER, utilized in this thesis is presented. Finally, the methods for defining the hydraulic correlations with Koch-Glitsch software are examined.

The KG-TOWER software does not concern foaming in any way. Since there was very little information about modelling of the foaming available in the field's literature, it was decided not to include modelling of the foaming in this thesis

4.1 Current distillation model in ProsDS

ProsDS is a dynamic simulation software developed by Neste Jacobs and is designed for building and simulating automation and process models. ProsDS is mainly used for process design studies and operator training. The development of ProsDS is carried out by using the integrated development tool LispWorks.

The distillation model in ProsDS consists of so called stirred tanks and possibly heat-exchangers. The stirred tank is a basic process tank corresponding to a flash drum. It consists of one calculation element. It is able to split the contents into phases and can also be set to apply heating or cooling duty. The heat-exchanger is a combination of two stirred tanks, between which energy can flow through a specific heat-exchanger area.

There is a standard distillation column model in ProsDS. Adding a distillation column to a process model starts with column initialization, in which the physical properties of the column, possible attachments and basic controls can be determined. The same column initialization menu can be used both for tray and for packed columns, as the mod-

elling depends only on the number of the calculation elements and the efficiency of the trays. In distillation modelling, the number of the calculation elements is the same as the number of the trays in the modelled column. The calculation elements are made unideal by setting the value of VLE efficiency smaller than 1. The dynamics of the model is thus closer to the one of the real process than if adding fewer ideal calculation elements. [6] In Figure 4.1 a distillation column model in ProsDS is presented.

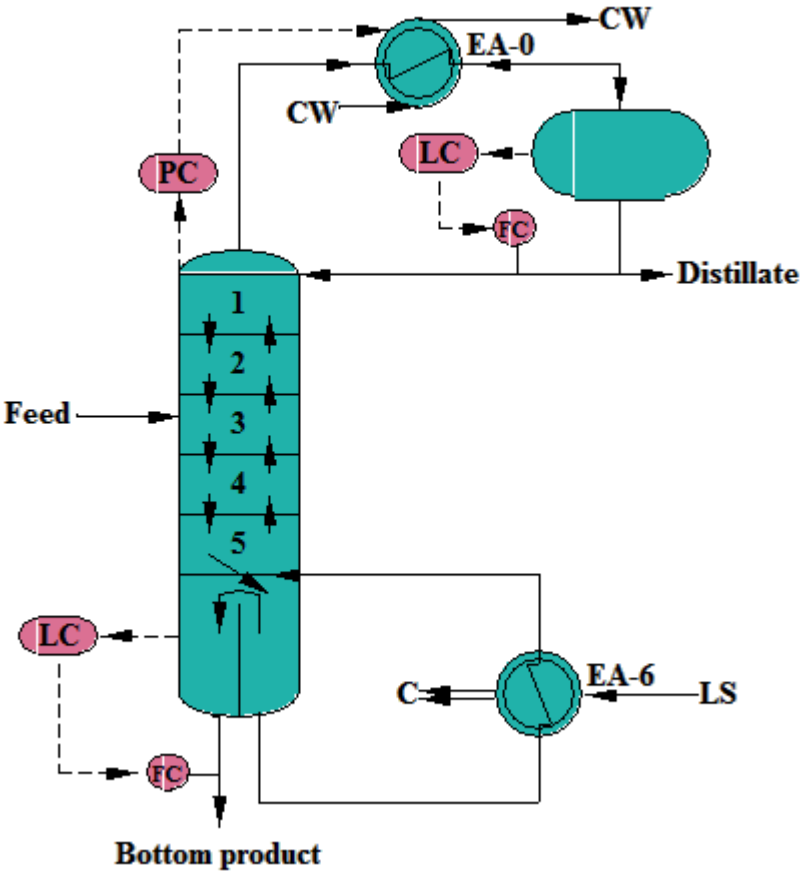

Figure 4.1. *A distillation column in ProsDS.*

In Figure 4.1 a distillation column model with five trays can be seen. There is also a reboiler, a condenser and an overhead drum included. In addition, the basic controllers of distillation columns, such as a level controller *LC*, a flow controller *FC* and a pressure controller *PC*, can be observed from the figure.

In the column initialization menu the thermodynamics used in the column, the physical sizing of the column, the number of the calculation elements and the separation efficiency are specified. Furthermore, the trays for the feed streams and side draws are specified. The equation of state used in vapor or liquid phases can be chosen to be ideal, Soave-Redlich-Kwong (SRK), Peng-Robinsin (PR) or user identified. Usually, the number of calculation elements in the modelled column is defined to be the same as in

the real column and the separation efficiency is defined so that the compositions of the distillate and bottom product in the model correspond to those of the real column.

The type of the condenser can be chosen as the condenser can be cooled by water, other liquid or air. The overhead drum and the controllers of the upper part of the column can be determined according to the case in question. If the overhead drum is not flooded, usually the overhead level is controlled with the reflux or distillate rate and the pressure is controlled with vapor outlet. If the overhead drum is flooded the pressure is controlled with the reflux or distillate rate, i.e. the level of the condenser. In the reboiler, the heating medium can be vapor or liquid. The reboiler duty is controlled with the heating medium rate.

Most parameters can be redetermined afterwards in the model. These parameters are column diameter, weir height, tray spacing, separation efficiency and thermodynamics used in the column. In addition, the condenser, reboiler and overhead properties can be changed after creating the column model. In addition, all controllers can be added or removed from the model whenever needed. That is, the number of trays is the only determination that cannot be automatically changed after the column is created.

The program automatically makes default definitions for inner vapor and liquid flows of the column. Definitions are always case-specific depending on the needs of the pressure calculation and the construction of the overhead. Definitions can be changed manually. The default definition for vapor flow is *Line Backward* in which case pressure information is transferred backward in the column from top to bottom. In line mode, all available flow is passed through the line without restrictions. The default definition for liquid flow is *Fill.* The liquid volume exceeding a specified level of the calculation element, meaning the height of the weir, is transferred to the lower calculation element. The amount of flow depends on the connection level of the lower calculation element. If the liquid level of the lower calculation element remains under the connection level, the flow is not restricted, but if the liquid level reaches the connection level, the rate flow entering the calculation element cannot exceed the flow rate leaving from the calculation element. In distillation column models, the connection level is usually 1, that is, the liquid from the higher calculation element flows to the top of the lower calculation element and the calculation element has to be full before the flow entering it is limited.

The hydrostatic pressure in the column is resulting from the height of the weir. The pressure drop is caused as the vapor flows through the liquid volume. There can also be pressure loss added to vapor flows presenting the dry pressure drop. The vapor flow leaves from the top of the calculation element and enters the bottom of the calculation element above. The liquid flow passes over the weir and drops into the top part of the calculation element below. [6] In Figure 4.2 a schematic of the current distillation model in ProsDS is presented. Each tray is modelled with one stirred tank.

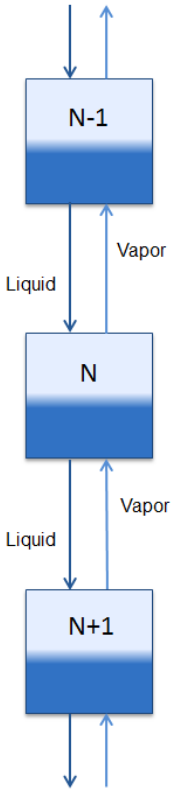

Figure 4.2. *A schematic of the current distillation model.*

In a current distillation model, flooding may occur. If the liquid height on the tray equals the tray spacing, all the liquid from the tray above will no longer flow to the tray below and liquid begins to accumulate to the tray above. As shown in Figure 4.2, each tray is modelled with one stirred tank and the active area and the downcomer are not separated. As a consequence, downcomer backup effect cannot be illustrated. For the same reason, it is also not possible for weeping to occur. As there is no liquid flow to the tray above, jet flooding cannot occur in the model. In addition, downcomer choke flooding is not possible to appear in the current distillation model, since there is no limitation for liquid flow to the tray below.

4.2 Koch-Glitsch KG-TOWER software

KG-TOWER software is a software program for sizing tray and packed columns. It is developed by the tray and packing manufacturer and vendor Koch-Glitsch. With the program, conventional and high performance valve trays as well as random and structured tower packings can be rated. The KG-TOWER software version 5.2 is used in this thesis.

When rating a column, first step is to enter the internal vapor and liquid rates and densities in the software. Vapor and liquid viscosities and liquid surface tension should be entered if they are known. In addition, the system factor presented in Table 3.1 is entered. It is possible to observe up to five cases with different loadings at the same time.

After entering the loading information, it is possible to select either tray or packing design. The second step requires entering the tray information. Tray type is chosen from the list and tower diameter and number of passes are entered. The valve type is chosen and valve quantity is determined along with tray spacing. After entering downcomer and weir geometry information, the results can be seen.

The results given by KG-TOWER are presented in Table 4.1. The quantities of the results and in which units are they reported are shown in the table. There are some recommendations on some of the result values, as preferred maximum or minimum values. They are also shown in the table.

Table 4.1. *Tray results of KG-TOWER software.*

Tray Results	**Unit**	**Recommended limit**
Jet Flood	%	max 85 %
Downcomer Flood	%	max 85 %
Downcomer Backup	mm liq / % (TS+W)	max 40 %
Dry Tray Pressure Drop	mm liq	max 15 % of tray spacing
Total Tray Pressure Drop	mm liq	
Head Loss Under DC	mm liq	1.5−25 mm
Turndown	%	min 50 %
Downcomer Exit velocity	m/s	max 0.46 m/s
Cf Active Area	m/s	
Weir Load	$m^3/h/m$	max 75−90 $m^3/h/m$
Weir Crest	mm liq	min 6 mm
Equation 13	%	
DC Residence Time	s	
DC Loading	$m^3/h/m^2$	
Blow Rating	%	
System Limit	%	
Unit Reference	%	

Jet flood and *downcomer flood* are reported as a percentage of the predicted point at which massive liquid accumulation will occur. Downcomer flood represents the choking effect at the entrance of the downcomer. *Downcomer backup* is reported in both millimeters of liquid and as a percentage of the tray spacing plus weir height. *Dry tray pressure drop* provides a relative indication of vapor velocity through the valves. For *Total pressure drop,* usually there is no specific limit on. *Head loss under the downcomer* is based on the downcomer clearance and the shape of the downcomer edge. *Turndown* is an approximation of the minimum vapor rate required for efficient tray activity. *Downcomer exit velocity* is the liquid velocity as it flows horizontally through the downcomer clearance. *Capacity factor* C_f is commonly a used density-corrected vapor velocity term on a per unit active area basis and is calculated according to the

equation (14) presented in the previous chapter. *Weir load* is generally used to determine the liquid load of the tray. *Crest* is the theoretical height of clear liquid flowing over the outlet weir and is directly associated with weir loading. *Equation 13* is the conventional valve tray jet flood capacity model from Glitsch Design Manual. There are also some results as the residence time in the downcomer, the downcomer loading, the blow rating, the system limit and the unit reference, but they are not relevant in this thesis. [32]

4.3 Determining hydraulic correlations

Determining the correlation between vapor and liquid flows and the tray hydraulics requires examination of results with several different vapor and liquid loads. With these different cases, the correlations between vapor flow and jet flooding as well as liquid flow and downcomer choke flooding and downcomer backup can be made. With made correlations, the limit value for the appearance of each phenomenon can be defined. The limit values for jet flooding and downcomer choke flooding can be determined according to limit value of 85 %. The limit value for weeping can be determined by multiplying the turndown ratio and the vapor rate. For the downcomer backup there is no need for defining a certain limit value, since as a phenomenon, it does not begin or stop at a certain loading, but is constantly occurring. The values at which the maximum jet flooding and maximum downcomer choke flooding are reached can be determined according to the value of 100 % of flooding.

As the limit values are defined, the correlations for liquid flow in jet flooding and weeping and downcomer choke flooding can be made. Jet flooding begins to occur, if the vapor rate exceeds a certain limit. At a certain point, all of the liquid fed to the tray is carried to the tray above. The function representing the correlation between the vapor rate to the tray and liquid rate carried to the tray above, is valued as zero as the vapor rate remains under the defined value. After that, simplified, the function is a linear correlation and reaches its maximum value at the defined value of 100 % of jet flood. In Figure 4.3 correlation for jet flooding in principal is presented.

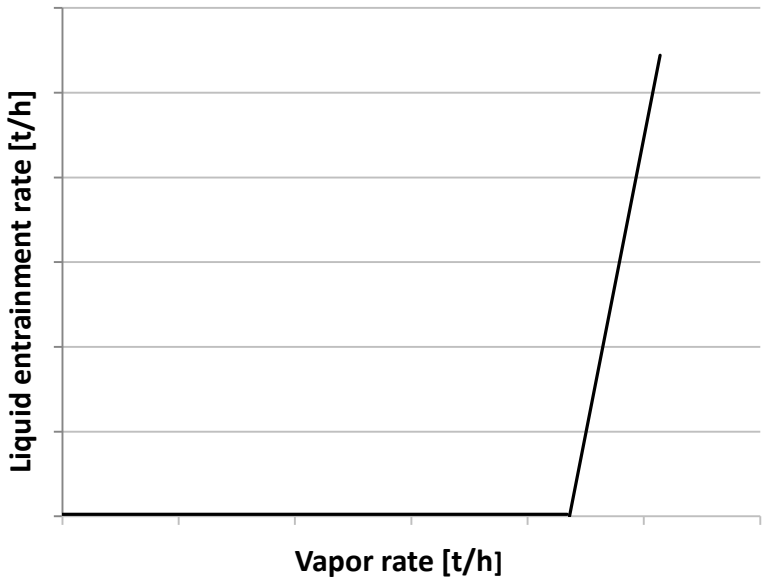

Figure 4.3. *General correlation form for jet flooding.*

The correlation for jet flooding can be presented as an equation. The liquid entrainment rate L_{jet} is represented as a function of vapor rate entering the tray in the following equation.

$$L_{jet} = \begin{cases} 0, & V < V_{lim,jet} \\ -\frac{L_{max,jet}}{V_{max,jet} - V_{lim,jet}}(V - V_{lim,jet}), & V \geq V_{lim,jet} \end{cases} \quad (22)$$

In the equation, L_{jet} is the liquid entrainment rate, $V_{limit,jet}$ is the limit value for vapor rate in jet flooding (85 % of jet flood), $V_{max,jet}$ is the vapor rate at which the maximum jet flooding occurs (100 % of jet flood) and L_{max} is the maximum entrainment rate. As in jet flooding at the maximum vapor rate, all of the liquid fed to the tray is carried to the tray above, the maximum entrainment rate is the current liquid flow entering the active area from the downcomer. Thus, the value of the maximum liquid entrainment rate and the value of the equation (22) depend on the amount of the liquid flow from the downcomer to the active area.

Weeping occurs if the vapor flow holding the liquid on the tray decreases under a certain point. If no vapor flows through the tray, all the liquid fed to the tray weeps to the tray below. Thus, it can be determined, that simplified, there is a linear function that represents the correlation between vapor flow and wept liquid flow. The function reaches its maximum value when the vapor flow is zero, and is valued as zero, if the vapor flow exceeds the defined limit value. In Figure 4.4 the general correlation for weeping in principal is presented.

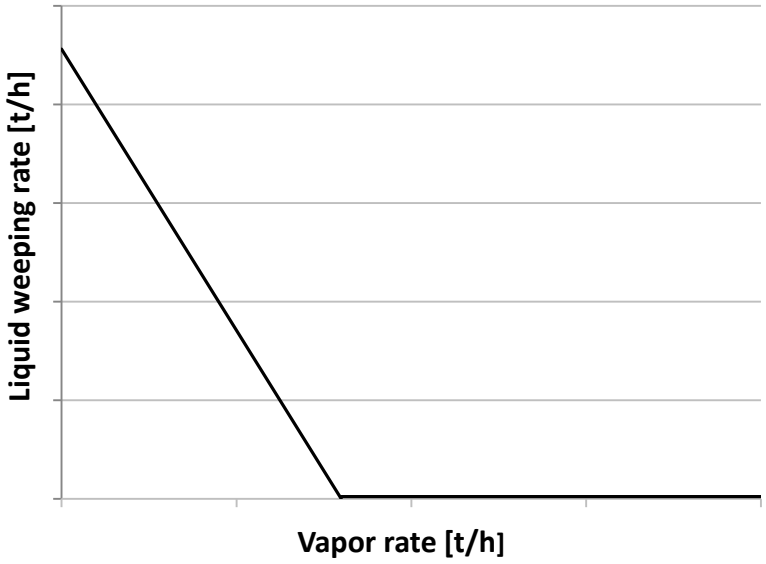

Figure 4.4. *General correlation form for weeping.*

The weeping correlation can be presented as an equation. The liquid weeping rate L_{weep} is represented as a function of vapor rate entering the tray in the following equation.

$$L_{weep} = \begin{cases} -\frac{L_{max,weep}}{V_{lim,weep}} * V + L_{max,weep}\,, & V \leq V_{lim,weep} \\ 0, & V > V_{lim,weep} \end{cases} \tag{23}$$

In the equation, V is the vapor rate entering the tray and $V_{limit,weep}$ is the limit value for vapor rate in weeping. The maximum weeping rate L_{max} can be calculated from the flow coefficient equation. As the flow coefficient remains constant, the value of the maximum weeping rate depends on the pressure loss and density of the weeping liquid flow. The higher the liquid level on the tray is, the greater the weeping flow rate is. Thus, the value of the maximum weeping liquid flow rate varies according to the pressure loss and density and, at the same time, the value of the correlation of the equation (23) varies.

In downcomer choke flooding when a large liquid flow rate is attempting to flow to the downcomer, the mouth of the downcomer can act as a restriction to flow and so require an increase in the froth height on the tray in order to achieve the required flow rate. The phenomenon can be presented with three functions. If the liquid flow rate from the active area to the downcomer remains under the limit of 85 % of downcomer flood, the flow is not restricted. Nevertheless, the liquid flow becomes limited as it exceeds the defined value of 85 % downcomer flood. After exceeding the value of 100 % downcomer choke, the liquid flow is entirely restricted to a constant value that is decided to be 90 % of the maximum value of downcomer choke. In Figure 4.5 the correlation for downcomer choke flooding is presented in principal.

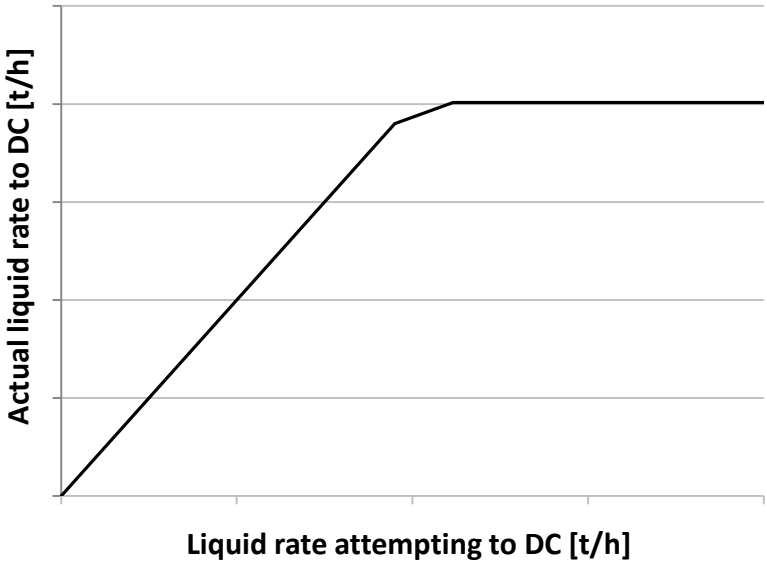

Figure 4.5. *General correlation form for downcomer choke flooding.*

In Figure 4.5 the actual liquid flow passing the mouth of the downcomer is presented as a function of the liquid flow attempting to downcomer. As there is no limitation for liquid flow before the certain limit, the angular coefficient of the function is valued as 1. This signifies, that all liquid rate attempting to the downcomer is also flowing to it.

The correlation for downcomer choke flooding consists of three parts. The actual liquid flow rate L_{choke} from active area to downcomer can be presented as

$$L_{choke} = \begin{cases} L_{att}\,, & L_{att} < L_{lim} \\ \frac{0.9*L_{max,choke}-L_{lim}}{L_{max,choke}-L_{lim}} * (L_{att} - L_{lim}) + L_{limit}\,, & L_{lim} \leq L_{att} < L_{max,choke} \\ 0.9 * L_{att}\,, & L_{att} \geq L_{max,choke} \end{cases}, \quad (24)$$

where L_{att} is the amount of the liquid flow attempting to flow to the downcomer, L_{lim} is the limit value at which the liquid flow is first limited (85 % of downcomer flood) and $L_{max,choke}$ is the liquid value at which the liquid flow becomes limited to a constant value (100 % of downcomer flood). The value of the liquid flow attempting to flow from active area to the downcomer can be calculated from the mass balance of the active area and is thus conditional on the flows entering and leaving the tray and the liquid accumulation on the tray.

5. IMPLEMENTATION OF THE HYDRAULIC CALCULATION

The improvement of the distillation model began with determining the structure of the new model. It was also considered, how the hydraulic constraints appear in the model and which flows needed to be added to the model. For determining the hydraulic correlations the KG-TOWER software was utilized.

The function of the developed model was first tested with a small ProsDS model of five separation elements and fixed pressure. The flow rates, pressures and levels of the tanks were also calculated manually with a spreadsheet and the simulation results were compared to those to verify the validity of the test model. After that, the calculation of the hydraulic correlations was implemented in the simulator by programming.

For more extensive examinations, the model was implemented in a distillation game. The model of the distillation game was rebuilt with the model structure developed in this thesis.

5.1 Development

The KG-TOWER software was utilized for determining the limit values in the correlations of jet flooding, downcomer choke flooding and weeping. Figure 5.1 shows the procedure of defining the limit values and flow coefficients that are needed in ProsDS, before the developed model can be used.

First, the tray geometry and loading information at several operating points need to be added in the KG-TOWER software. From the results of the software the limit value for weeping can be calculated based on the turndown ratio. For jet flooding and downcomer choke flooding, linear functions can be formed based on the results of different loadings. From the linear functions, limit values of 85 % and 100 % i.e. the start point of flooding and the point of maximum flooding can be defined. With these limit values, the correlations for jet flooding, downcomer choke flooding and weeping can be defined.

The ProsDS model also uses flow coefficients in vapor flows and liquid flows from the active area to the downcomer. In vapor flow the flow coefficient represents the dry pressure drop and in liquid flow the head loss under the downcomer. The values of the flow coefficients can be defined based on the KG-TOWER results.

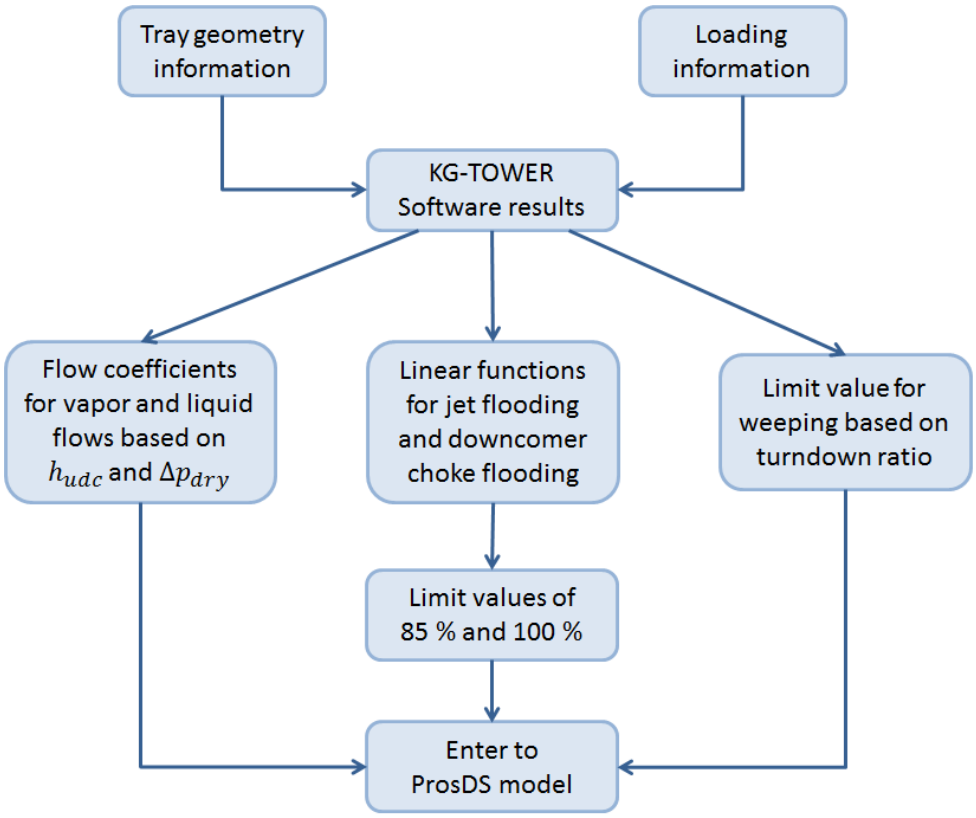

Figure 5.1. *The steps involved in defining the needed values to a ProsDS model.*

In this subchapter, first the developed model structure is described. Then, some special tray constructions are considered. In addition, the defining of the correlations for jet flooding, downcomer choke flooding and weeping and the built ProsDS test model of five separation elements and fixed pressure are presented. Finally, the simulation results of the model are examined.

5.1.1 Model structure

Since the current distillation column model cannot model the tray hydraulics due to its structure of one stirred tank representing each tray, it was essential to reconsider the structure of the model. It was decided to separate the active area and the downcomer of a tray to separate stirred tanks instead of one stirred tank representing each tray. In this way, the realization of all hydraulic constraints was possible. In Figure 5.2 the schematic of the improved distillation model compared to the function of a tray column is presented.

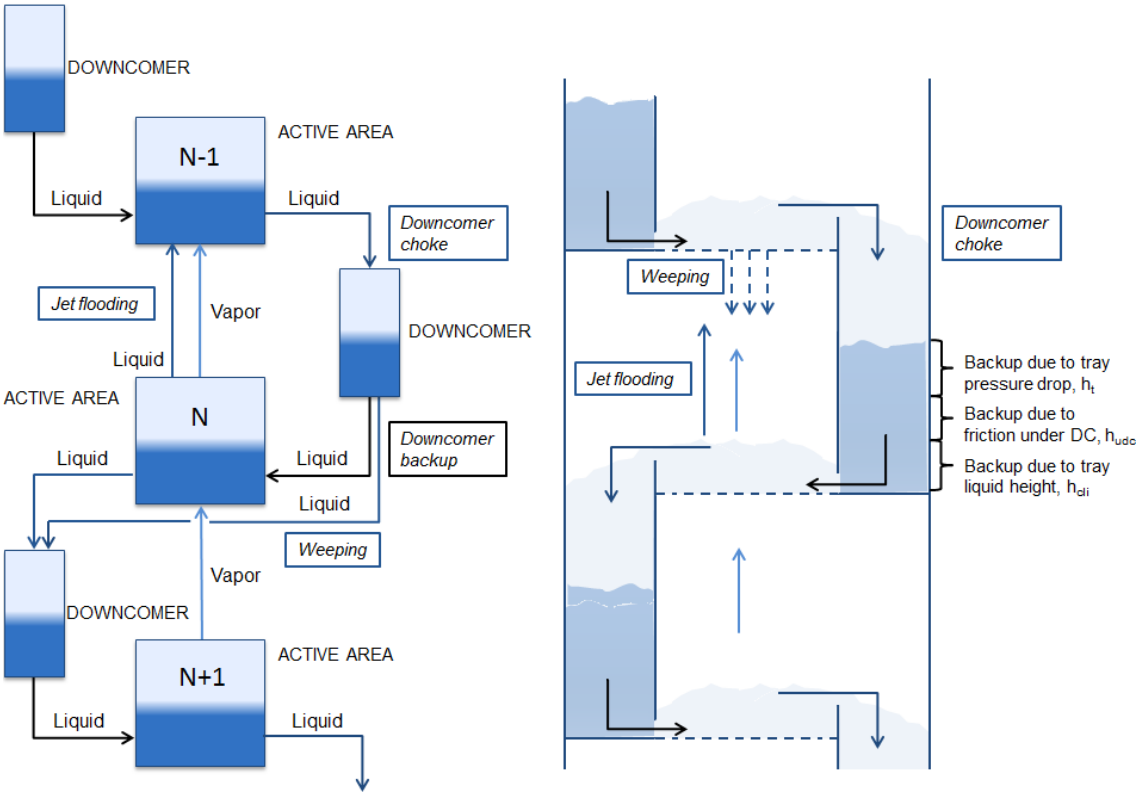

Figure 5.2. *Schematic of the improved distillation model.*

In Figure 5.2, the tanks representing the active areas and the downcomers as well as the vapor and liquid flows between them are presented. In addition, the scene of the each hydraulic phenomenon is shown. To represent all hydraulic phenomena, some liquid flows needed to be added to the model. In jet flooding, the liquid from the tray is carried to the tray above. Thus, for jet flooding there needs to be a liquid flow from the active area *N* to the one above. In weeping the liquid flows through the active area to the tray below. In reality, weeping may occur across the whole active area. If the liquid weeps through the tray straight after the downcomer, it bypasses basically two active areas, the one it weeps from and the one it weeps to. Instead, if the liquid weeps just before the outlet weir, it does not bypass any active areas. There is a liquid gradient on the tray and for that there is more liquid on the tray right after the downcomer than just before the outlet weir. Consequently, as the vapor flows more easily through the liquid of lower level, the weeping is more probable to occur right after the downcomer. Nevertheless, in this thesis it is assumed that as an average, liquid bypasses one active area. Thus, for weeping, there is a liquid flow from the downcomer *N-1* to the downcomer below, and so one active area is bypassed. The structure of separate stirred tanks for an active area and for a downcomer enables the downcomer backup and downcomer choke effect to occur according to the configuration and do not require any additional flows to the model. In the schematic of the improved distillation model shown in Figure 5.2 jet flooding concerns the tray *N*. Downcomer choke and downcomer backup as well as weeping are the phenomena of the tray *N-1*.

5.1.2 Special tray constructions

The distillation model presented above is developed for tray columns in general. The model can be applied for several tray constructions. For valve and sieve trays the model is valid as it is. If the modelled column consists of bubble-cap trays, the weeping liquid flow will be valued as zero since bubble-cap trays cannot weep.

Liquid and vapor feeds can be added to the model. The liquid and vapor feeds are usually fed to an active area. What need to be considered when adding a feed flow to the model, is that the liquid and vapor feeds are added to the correct trays. In an actual distillation column if the vapor-liquid mixture is fed to the tray, liquid flows down to the active area, but vapor flows up to the tray above. The vapor fed to the tray does not interact with the liquid on the tray but the liquid on the tray above. Consequently, in the model, separate liquid and vapor feeds are required and the vapor needs to be fed to the bottom of the tray above the tray in which the liquid is fed. In Figure 5.3 vapor and liquid feeds are presented.

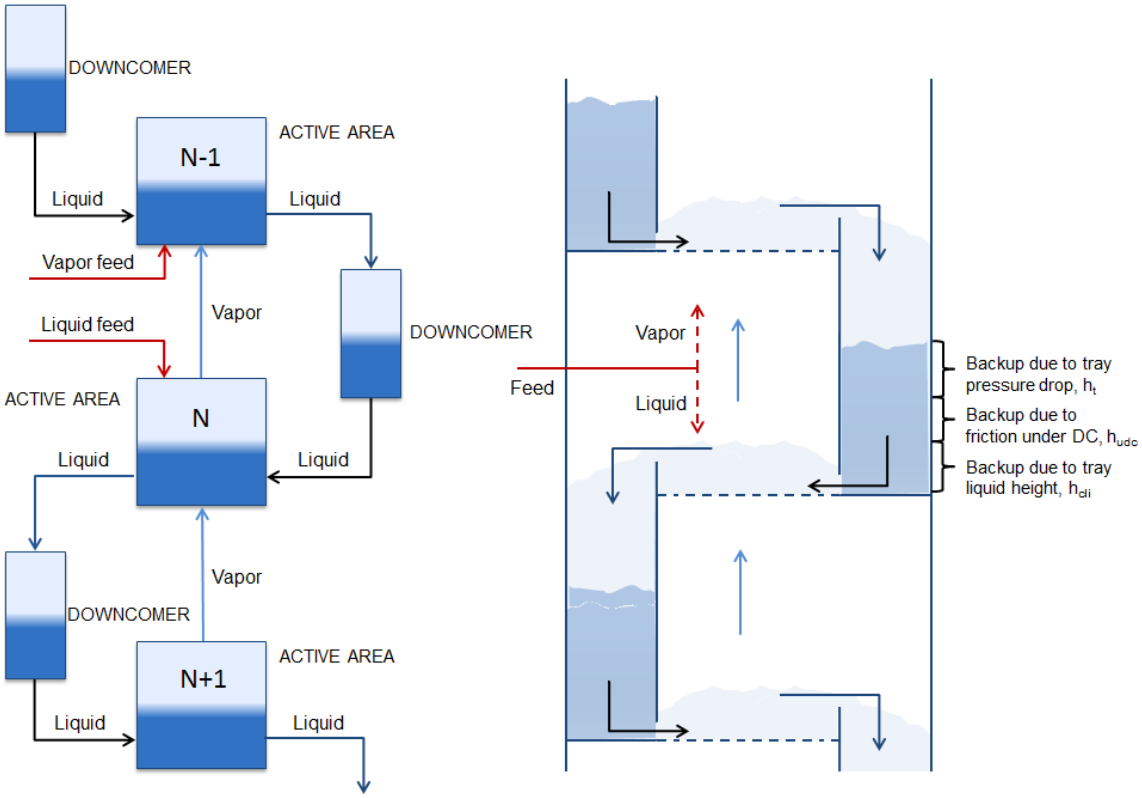

Figure 5.3. *Vapor and liquid feeds.*

Vapor is not often withdrawn from the column, but in the model a vapor draw-off can be added to the top part of the active area. Chimney trays are often used for withdrawing intermediate liquid streams from the column. Chimney trays are preferred especially when all liquid in a column section is withdrawn. Alternative devices used for liquid

withdrawal are downcomer trapouts. They are mainly used for partial liquid draw-off from tray columns. [15, pp. 103−111]

In the model liquid can be withdrawn partially or totally from a column section. In chimney trays, the vapor and liquid are not in contact on the tray the liquid is withdrawn from and the composition of the withdrawn liquid is near the composition of the liquid in the downcomer above. Therefore, in the model the liquid draw-off cannot be added to the active area, but to the downcomer above. In that way, liquid is not in contact with vapor in the model. As the liquid is withdrawn totally, there is no liquid flow to the active area below, unless there is a feed or reflux flow to that tray. In Figure 5.4 total draw-off from the column are presented.

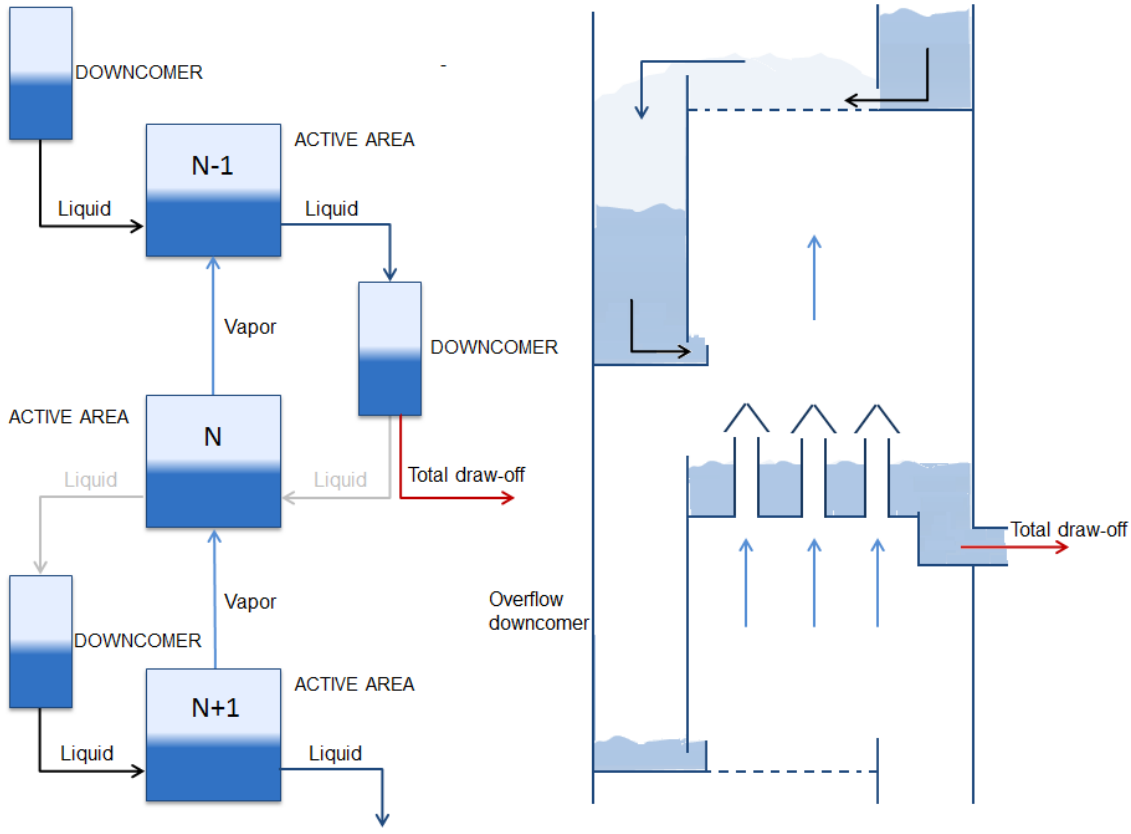

Figure 5.4. *Total draw-off from column section.*

In chimney trays, the liquid level can exceed the height of the chimneys and consequently the liquid will flow to the overflow downcomer and from there to the active area below. In the model, the liquid flow from the downcomer to the active area can be defined to leave the downcomer from the height of the chimneys. Thus, if the liquid level exceeds the height of the chimneys the liquid will flow to the active area below. Downcomer trapouts are used for partial draw-off from the distillation column. In Figure 5.5 a partial draw-off from the downcomer is presented.

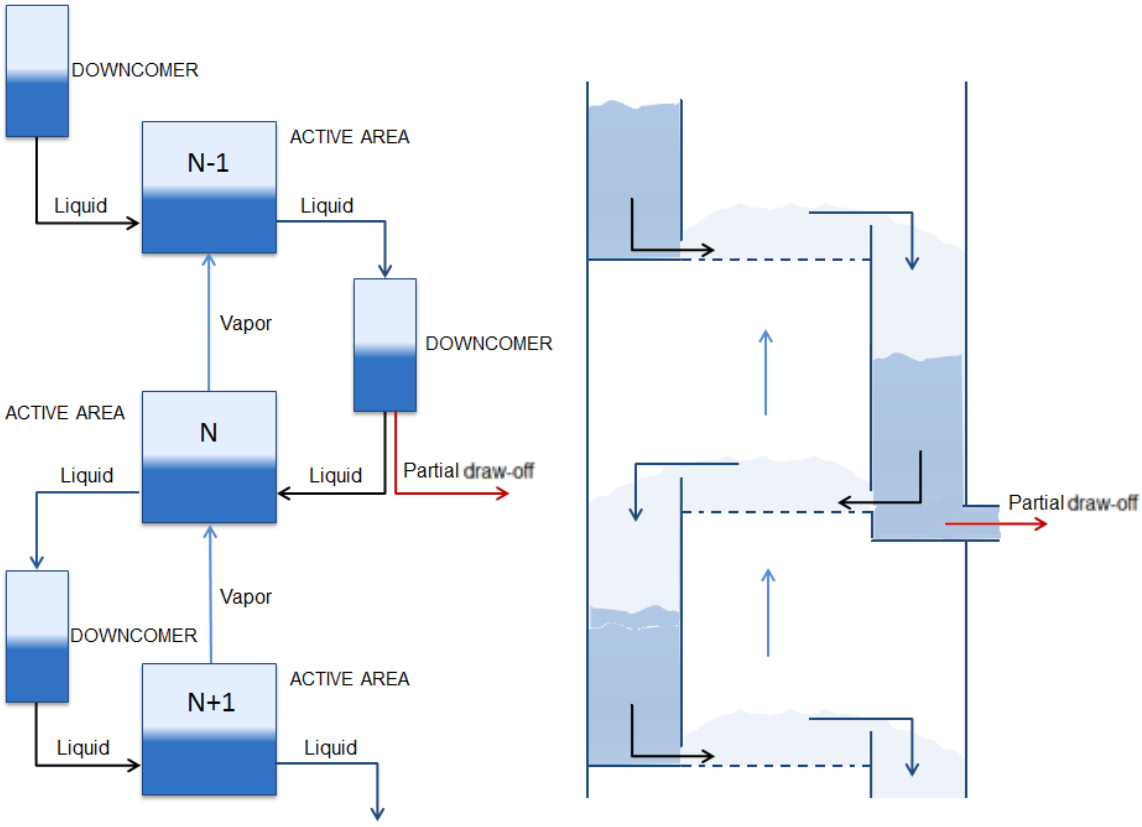

Figure 5.5. *Partial draw-off from column section.*

The partial draw-off is added to the bottom of the downcomer in the model. Because the liquid is only partially withdrawn, the liquid flow from downcomer to the active area continues but decreases as part of the liquid flow is withdrawn.

5.1.3 Correlation determining

For testing, the developed distillation model was applied to a top part of the dehexanizer column DA-10203 of the Porvoo refinery. First, the tray information with vapor and liquid loadings of normal operation as well as loadings of 60 %, 80 % and 120 % were entered to KG-TOWER software. The results of the software are presented in the appendix A. Linear functions for jet flooding percentage and downcomer choke flooding percentage were formed based on the result. In Figure 5.6 jet flooding percentage is presented as a function of vapor flow rate and in Figure 5.7 downcomer flooding percentage is presented as a function of liquid flow rate.

From the functions of Figure 5.6 and 5.7 the limit values of 85 % and 100 % of flooding were defined. For jet flooding the vapor flow limit values were 218 t/h and 257 t/h. The limit values of liquid flow in downcomer choke flooding were 190 t/h and 223 t/h. The limit value for weeping was calculated based on the result value of turndown ratio, that is, limit value for weeping equals the multiplication of vapor rate and turndown ratio. The limit value for vapor rate in weeping was 80 t/h.

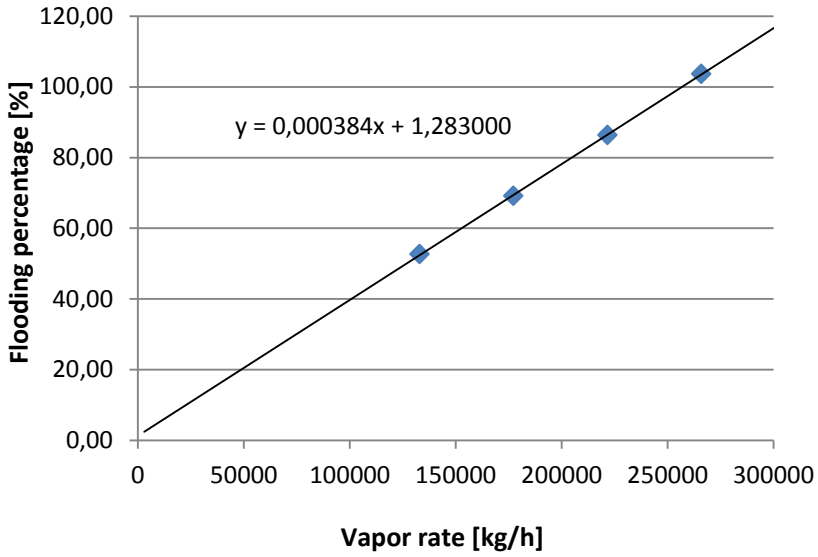

Figure 5.6. *Percentage of jet flooding as a function of vapor flow rate.*

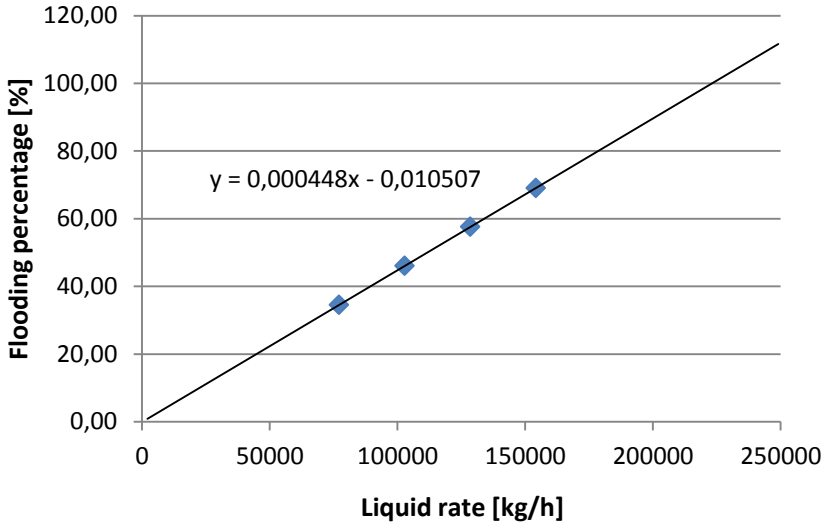

Figure 5.7. *Percentage of downcomer choke flooding as a function of liquid flow rate.*

After knowing the limit values for vapor and liquid rates, the correlations for jet flooding, weeping and downcomer choke flooding were defined according to equations presented in Subchapter 4.3 by placing the defined limit values to the equations (22), (23) and (24). The liquid entrainment flow rate in jet flooding was given by

$$L_{jet} = \begin{cases} 0, & V < 218 \\ -\frac{L_{max,jet}}{33}(V - 218), & V \geq 218 \end{cases}.$$

In weeping, the amount of the liquid wept from tray to one below could be calculated as follows.

$$L_{weep} = \begin{cases} -\frac{L_{max,weep}}{80} * V + L_{max,weep}\,, & V \leq 80 \\ 0, & V > 80 \end{cases}$$

In downcomer choke flooding, the actual flow rate entering the downcomer could be calculated based on the liquid attempting to flow the downcomer according to

$$L_{choke} = \begin{cases} L_{att}\,, & L_{att} < 190 \\ 0.33 * L_{att} + 128.39\,, & 190 \leq L_{att} < 223 \\ 0.9 * L_{att}\,, & L_{att} \geq 223 \end{cases}.$$

5.1.4 Model building

The model was built in ProsDS according to the developed model structure by using the stirred tanks. The stirred tanks were connected with vapor and liquid flows as showed in Figure 5.2. The model was first built with five separation elements and so that the liquid and vapor flows could be separately varied for making the testing of the model easier. In addition, the correlations were first built in the model with function blocks so that they could be easily modified. In Figure 5.8 the first version of the model is presented.

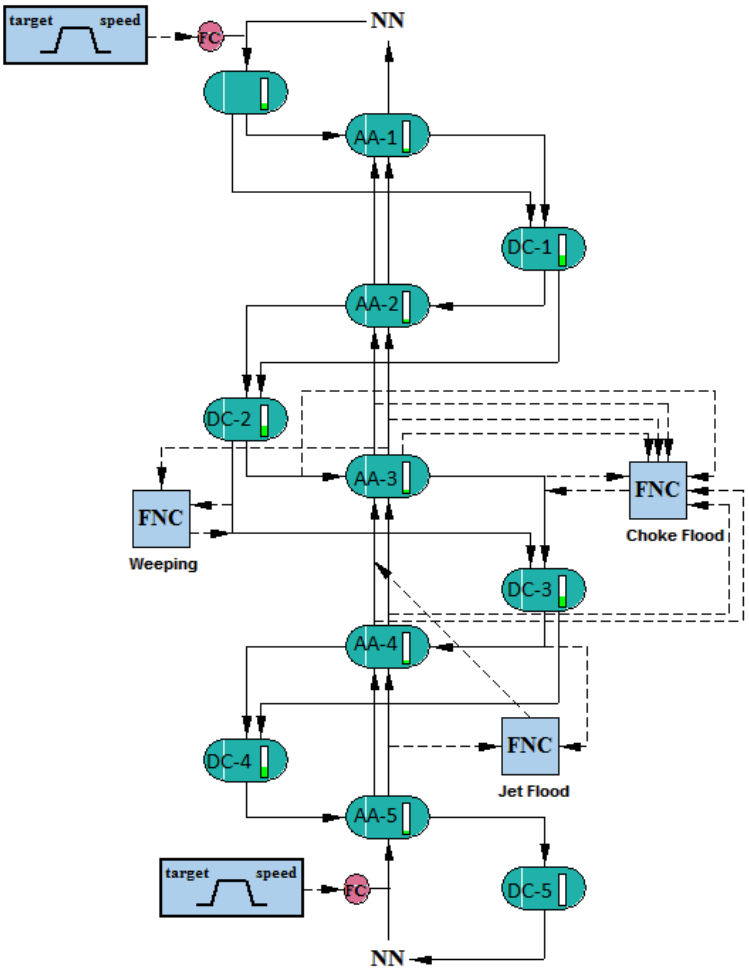

Figure 5.8. *First version ProsDS model for testing.*

Vapor flows from top of the active area tank to bottom of the one above. In vapor flow there is a flow coefficient representing the dry pressure drop. Liquid flows from the

weir height of the active area tank to the top of the downcomer tank, and from the bottom of that to the bottom of the active area tank below. The liquid flow rate from downcomer to active area is calculated based on the pressures at the downcomer bottom and the active area bottom. In the flow, there is also a flow coefficient representing the head loss under the downcomer. Values of the flow coefficients were defined based on the KG-TOWER results. The values of dry pressure drop and head loss under downcomer were utilized.

In the model, pressure propagation is backward from column top to bottom since pressure control of the column is usually in overhead drum. The downcomers are in the same pressure than the active areas above. The model calculates the downcomer backup according to total pressure drop, liquid height on the tray and head loss under the downcomer. As the liquid flow from active area to downcomer is defined so that, if the tank is full, the liquid flow entering the tank cannot exceed the liquid flow leaving the tank, the liquid starts to accumulate to the active area. Thus, downcomer backup flooding occurs. Correlations for jet flooding, weeping and downcomer choke flooding are determined in the model according to the ones presented in the previous subchapter. The liquid flow rates for jet flooding and weeping are controlled according to the correlations. The liquid flow from the active area to the downcomer is restricted according to downcomer choke correlation.

As liquid flows from the active area to the downcomer from the weir height, in weeping, the liquid level on the active area remains at the weir height. At zero vapor flow, the liquid flow from downcomer to the active area is zero, since all the liquid weeps and bypasses the active area. The liquid flow from the active area to the downcomer is thus also zero, since there is no liquid volume exceeding the weir height on the active area. In reality, when the feed is stopped and all the liquid has wept in the column, there are no liquid volumes on the trays. For emptying the active area tanks in the model, extra lines needed to be added from bottom of the active area to the top of the downcomer. The lines are controlled so that they are zero as long as there is any vapor or liquid flow to the active area. If there are not any other flows, the liquid volume from the active area flows to the downcomer and from there weeps to the next downcomer.

5.1.5 Testing

The geometry information of the trays, composition of the feeds and pressure and temperature values were determined in the model. The function of the all hydraulic constraints was tested by varying the liquid and vapor rates. The liquid flow rates, pressures and levels of the tanks in the simulation model were also calculated manually with a spreadsheet to verify the accuracy of the simulation model. In the spreadsheet calculations, the vapor flow to the bottommost tank and the liquid flow to the topmost tank were valued the same as in the simulation. In addition, the pressure and the level of the topmost tank were defined based on the simulation results. In the calculations, flashing

was not taken into consideration. Thus, it was assumed that all the vapor rates were equal to the vapor flow to the bottommost tank i.e. the mass flows of vapor and liquid were not mixed. Liquid fed to the topmost tank did either flow to the next tank or accumulate. In the calculations, the mass balance and flow coefficient equations were utilized. The calculations were repeated to all time steps of the simulation time. The results of some calculations for the first time steps are presented in the appendix B. The values that were defined based on the simulation results are marked with grey and the values that were calculated are marked with black. In addition, the equations used in calculations are shown in the appendix.

First, the downcomer choke flooding was tested. The liquid rate was increased rampwise from the value 119 t/h to the value 220 t/h. Both simulated and calculated liquid flow rates can be seen in Figure 5.9.

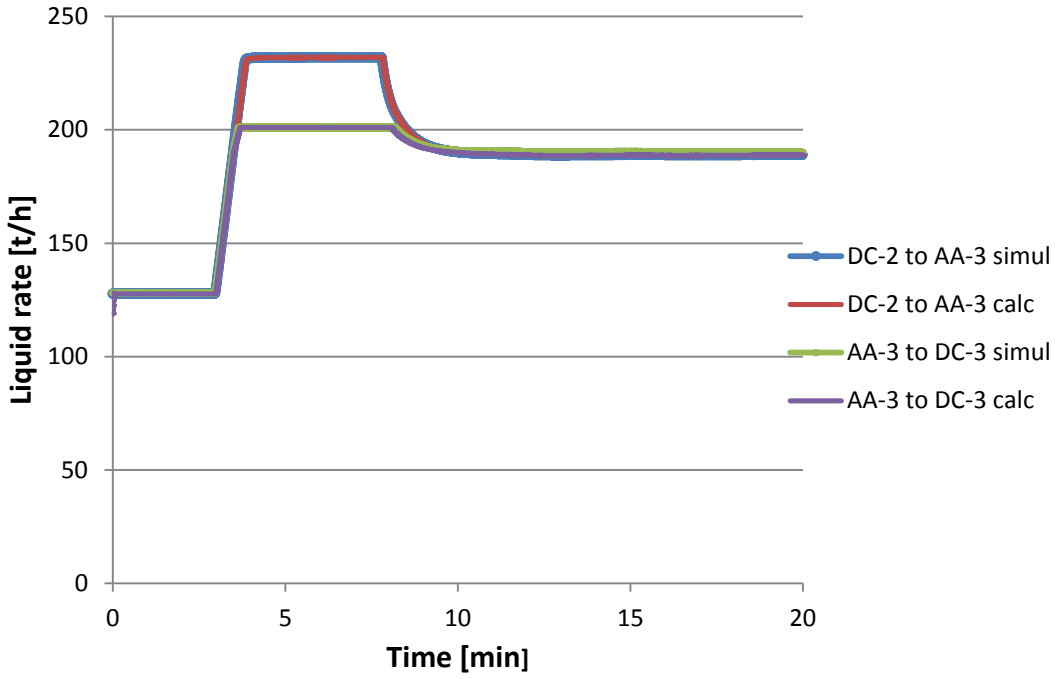

Figure 5.9. *Simulated and calculated liquid flow rates in downcomer choke.*

In the figure, downcomer choke effect can be seen. As the liquid flow rate from downcomer to active area increases, the liquid flow from active area to next downcomer is limited to a constant value. Since the liquid flow leaving the active area is less than the liquid flow entering the active area, the liquid starts to accumulate to tray which causes that the liquid flow entering the active area decreases. Consequently, the liquid flow rate from active area to the next downcomer also decreases. In Figure 5.10 the liquid heights on the active areas and downcomers are presented.

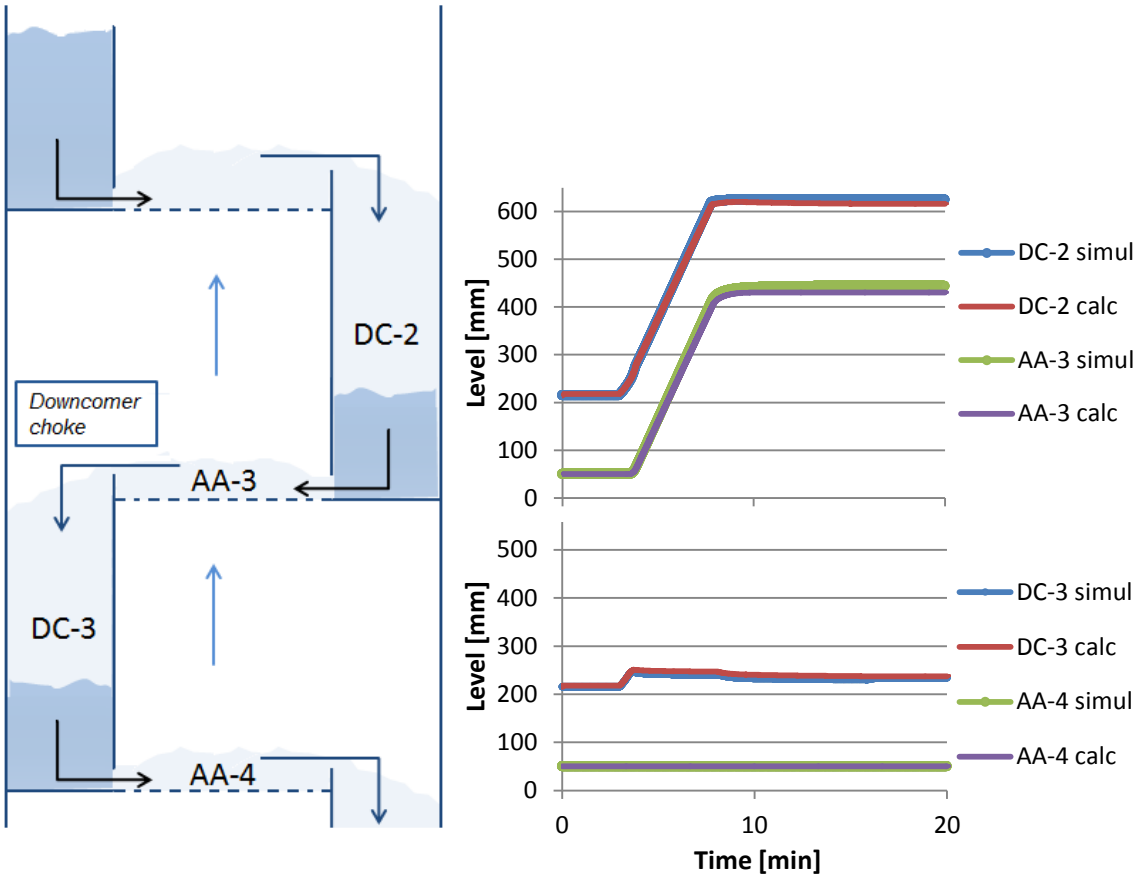

Figure 5.10. *Downcomer and active area levels in downcomer choke flooding.*

The figure shows that the liquid starts to accumulate to the active area and the downcomer above the limited flow as the downcomer choke effect occurs. The level of the downcomer which the limited liquid flow rate enters does not rise significantly and the level of the active area below remains constant, as the restriction of the flow was implemented only to one flow. The simulated and manually calculated results do not differ notable from each other.

Weeping was tested by decreasing the vapor flow from 235 t/h to 0 t/h. As explained in Subchapter 5.1, the actual weeping of a tray is modelled as a liquid flow from a downcomer to the one below. In Figure 5.11 the ramp-wise decreasing vapor rate is presented with liquid flow rates. As the vapor flow rate decreases to the limit value of 80 t/h, the weeping begins to occur. As the vapor flow rate stops, the weeping liquid rate reaches its maximum value which is the amount of liquid rate fed to the downcomer. The liquid flow fed to the downcomer where weeping occurs, remains almost constant apart from moderate varying during the vapor decrease. As the weeping flow rate increases, the liquid flow rate from downcomer to active area decreases, and at the zero vapor rate, all liquid fed to the downcomer weeps to the one below and no liquid enters the active area. In Figure 5.12 the simulated and calculated liquid levels of the column model are shown.

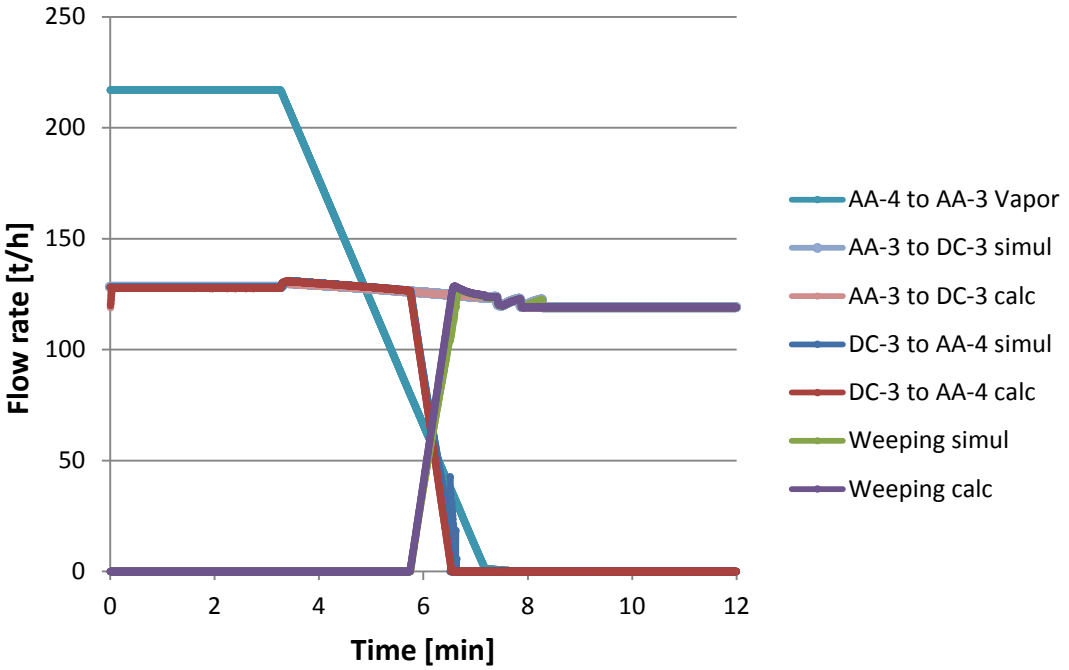

Figure 5.11. *Flow rates in weeping.*

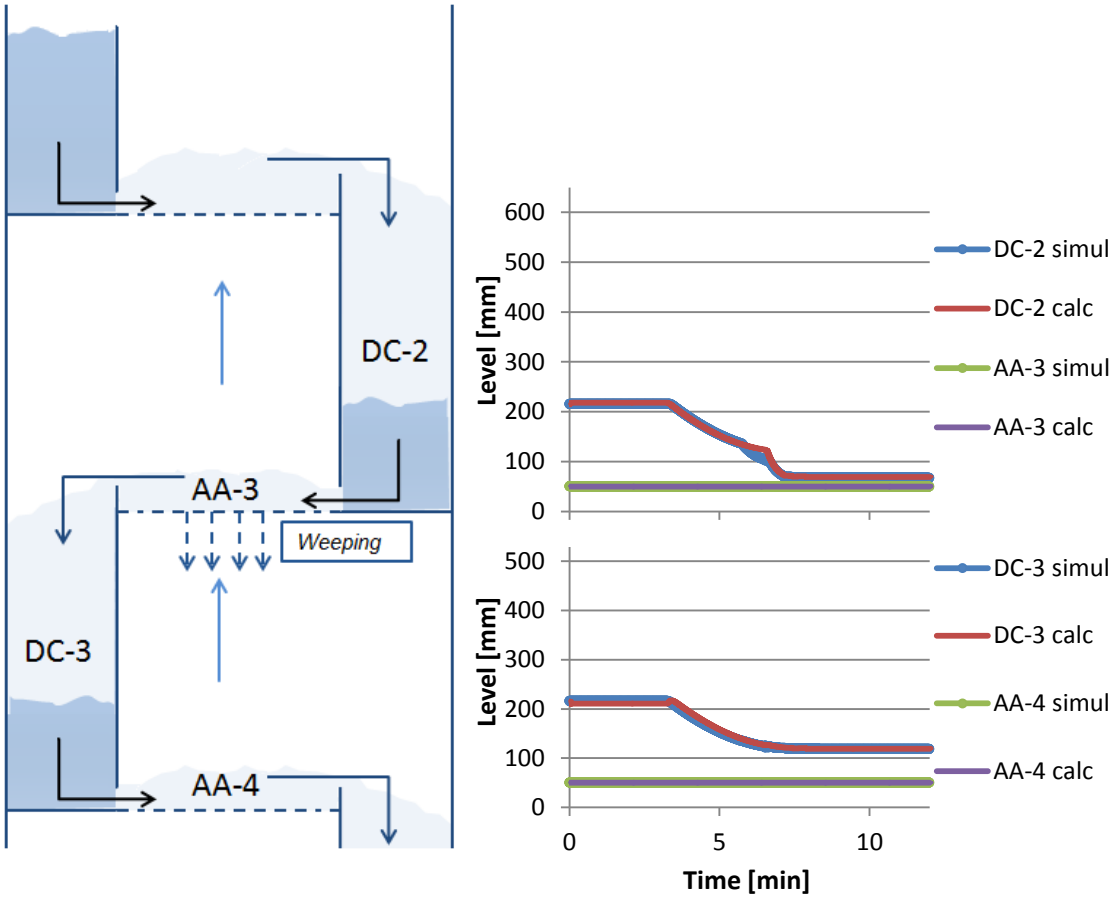

Figure 5.12. *Downcomer and active area levels in weeping.*

From Figure 5.12 it can be noticed that weeping does not affect the liquid heights on the active areas. In downcomers the level lowers as the dry pressure drop decreases due to vapor rate decrease. Consequently, the total pressure drop of a tray decreases affecting the liquid backup to the downcomer. The levels do not lower more due to constant liquid feed. The simulation and calculation results do not differ much from each other in weeping.

Lastly, jet flooding was tested. The vapor flow rate was increased ramp-wise from the value of 235 t/h to 280 t/h. In jet flooding, there is a liquid flow rate from the active area to the one above. As the entrainment liquid rate is added up to liquid rate entering the active area from downcomer, the liquid flow rate from the active area to the downcomer starts to increase massively. Nevertheless, the flow rate is limited by downcomer choke effect. Thus jet flooding and downcomer choke effect occur at the same time. In Figure 5.13 the increased vapor flow is shown with liquid flows. As the vapor flow reaches the limit value of 218 t/h, jet flooding starts to occur. At the same time, the liquid flow from the active area to the downcomer increases and when it reaches the choke flooding limit value of 201 t/h, the flow is limited to constant value. At the maximum vapor rate limit of 257 t/h, the jet flooding equals the liquid fed to the active area, that is, all liquid fed to the tray is carried away with vapor to the tray above. This can also be noticed by observing the liquid flow from the lower active area to the next downcomer, since after jet flooding starts to occur, the liquid rate from the active area to the next downcomer starts to decreases and is valued as zero as jet flooding reaches its maximum value. The upper active area and the downcomer start to fill, and due to the increased level of the active area, the liquid from the downcomer to active area decreases and stops.

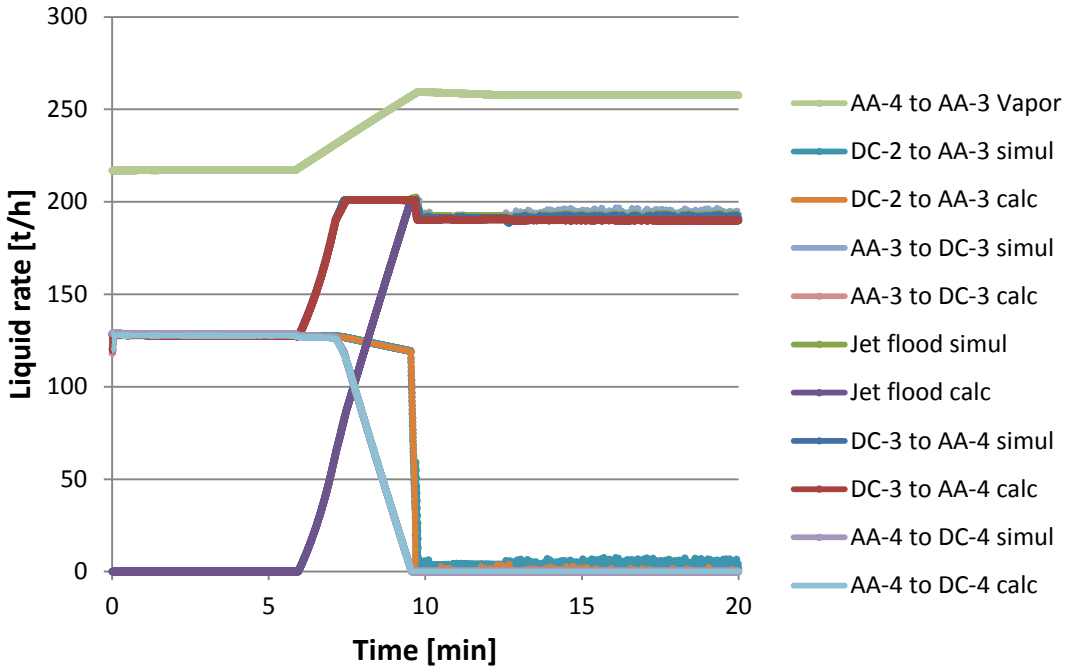

Figure 5.13. *Flow rates in jet flooding.*

In the Figure 5.14 the levels of the downcomers and active areas are presented in jet flooding. The level of the active area where the entrainment liquid is carried and the level of the downcomer above that, increase as jet flooding starts to occur. The downcomer becomes full of liquid so the liquid accumulation will also occur on trays above. The level of the downcomer through which the entrainment liquid flows increases a bit, as the amount of the liquid fed to the downcomer increases, but the downcomer does not fill more, since the liquid flow entering the downcomer is restricted. The level of the active area below remains on constant level.

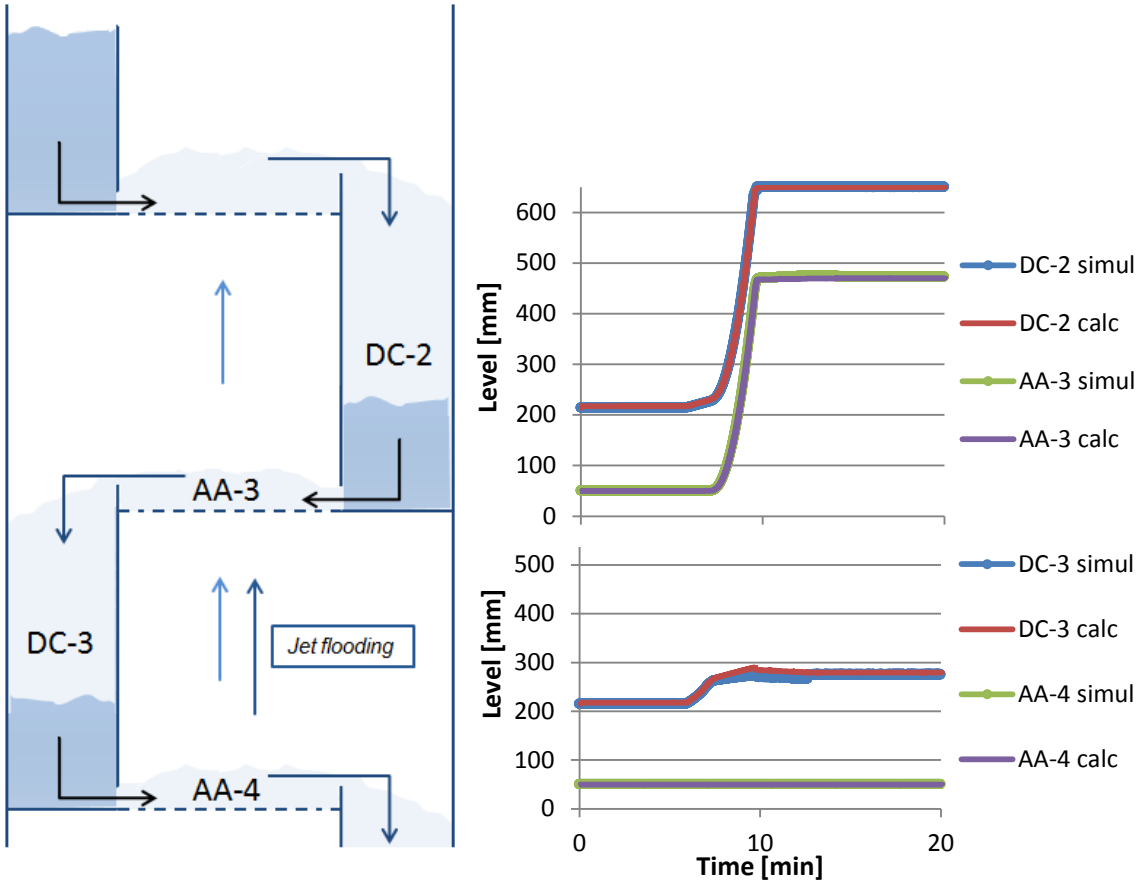

Figure 5.14. *Downcomer and active area levels in jet flooding.*

The simulated and calculated results of the jet flooding do not differ significantly from each other. However, at the second half of the simulation time, there are some oscillations in simulated liquid flow rates, whereas the calculated flows are constant.

After verifying that the simulation results equal the manually calculated results, all the hydraulic correlations were implemented in ProsDS by programming in ANSI Common Lisp. The programming was carried out by using the integrated development tool LispWorks 6.1.1 32-bit Professional Edition for Windows, which is also used in ProsDS development. In the code, mass flow for weeping and jet flooding flows and the value of maximum flow allowed for liquid flow from the active area to the downcomer are calculated in each time step according to current vapor and liquid flow rates.

5.2 Implementation

For more extensive examination of the developed hydraulic calculation, it was decided to implement the model in the distillation game. In Neste there are several different environments for focused training in use. These so called games are smaller entities than operator training simulators and with them more detailed observation of some part of the process, for example distillation or condensing, is possible. In games, there are different cases, in which typically something is changed, and the user gets points according to his corrective actions.

In the distillation game, the model is applied for the dehexanizer column DA-10203 of the Porvoo refinery. The current model of the distillation game uses the ProsDS distillation model in which there are no separate tanks for downcomers. It was decided to rebuild the model of the distillation game with the model structure developed in this thesis.

The process of the implementation of the distillation game model was similar to the test model. First, the KG-TOWER software was utilized for defining the limit values for jet flooding, choke flooding and weeping. Then, the model was built in ProsDS. Configuration of the model was more troublesome than the small test model. Before any hydraulic phenomena were added in the model, the distillation column was stabilized. After that, the defined limit values were entered to the model for the programmed hydraulic calculation. Finally, the function of the column with hydraulic phenomena was tested. In this subchapter, the correlation defining, the distillation game model and the simulation results of the model are presented.

5.2.1 Correlations

The tray information of the dehexanizer column DA-10203 along with vapor and liquid loadings of normal operation as well as loadings of 60 %, 80 % and 120 % were entered to KG-TOWER software. Since in the column there are different kind of trays in the top part of the column (trays 1…19) and in the bottom part of the column (trays 20…40), the information needed to be entered to the software separately for both column sections. As the trays in the column are special high performance trays, so called Superfrac trays, the software gave only the jet flooding percentage and the total tray pressure difference as a result. These results given by the software are presented in the appendix C.

For defining the limit values for downcomer choke flooding and weeping, Koch-Glitsch needed to be consulted. With the additional information received from Koch-Glitsch, the limit value for weeping was defined to be 30 t/h and it was same for the whole column. Linear functions for jet flooding percentage and downcomer choke flooding percentage were formed based on the software results and the received additional information. For jet flooding, the software gave a range for each loading rate. The linear

functions for jet flooding percentage were formed based on the average value of each range. In Figure 5.15 jet flooding percentage is presented as a function of vapor flow rate for the top and bottom parts of the column. For defining the linear function for downcomer flooding percentage, the additional information was utilized. Figure 5.16 downcomer flooding percentage is presented as a function of liquid flow rate for both top and bottom part of the column.

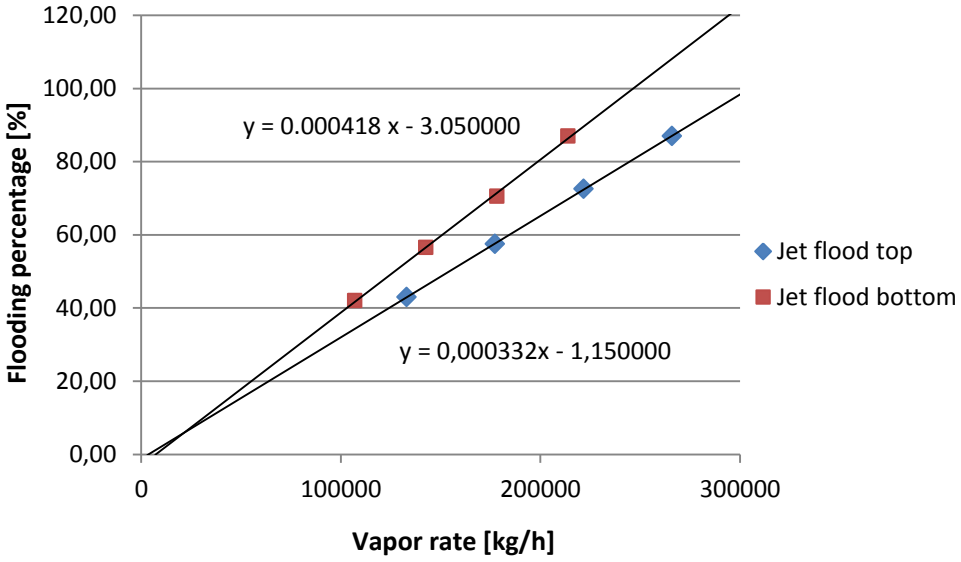

Figure 5.15. *Percentage of jet flooding as a function of vapor flow rate.*

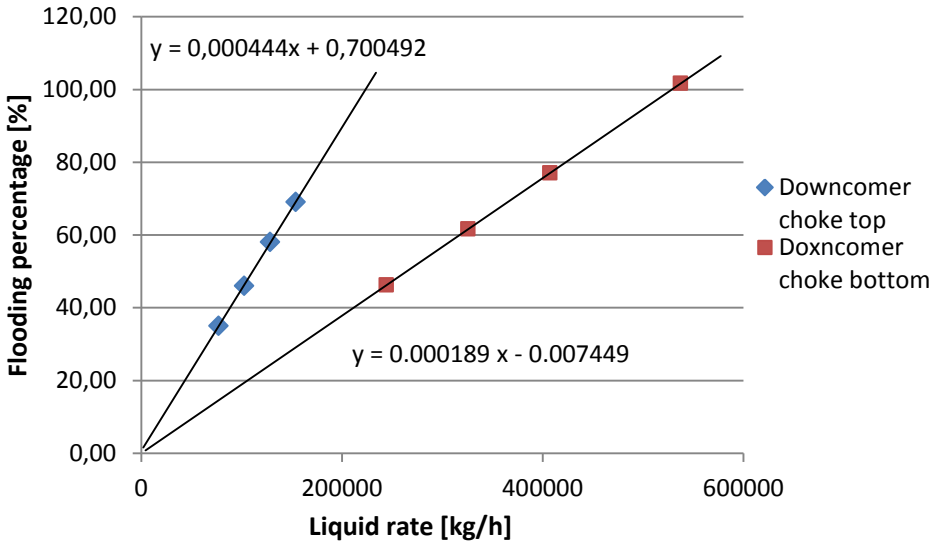

Figure 5.16. *Percentage of downcomer choke flooding as a function of liquid flow rate.*

From the functions of Figure 5.15 and 5.16 the limit values of 85 % and 100 % of flooding were defined. For jet flooding the vapor flow limit values were 253 t/h and 298 t/h for the top part of the column and 211 t/h and 247 t/h for the bottom part of the column. The limit values of liquid flow in downcomer choke flooding were 190 t/h and 224 t/h for the top part of the column and 450 t/h and 529 t/h for the bottom part of the column.

5.2.2 Model

The distillation model of the distillation game consists of a reboiler, a column, a condenser and an overhead drum. There are 40 trays in the distillation column. Liquid is fed to the tray 20. The geometry information of the active areas and downcomers as well as composition, pressure and temperature of the feed were determined in the model.

Since the overhead drum of the model is flooded, the pressure calculation in the model is in the condenser. ProsDS uses equation of state in pressure calculation, so the pressure calculation is preferred to take place in an object containing more vapor. The pressure propagation in the model is forward from condenser to overhead drum and backward from condenser to reboiler through the active areas. The downcomers are in the same pressure that the pressure at the weir height of the active areas.

The flows are defined the same way they are defined in the test model. Vapor flows from top of the active area tank to bottom of the one above. Liquid flows from the weir height of the active area tank to the top of the downcomer tank, and from the bottom of that to the bottom of the active area tank below. The liquid flow rate from active area to downcomer is defined so that, if the tank is full, the liquid flow entering the tank cannot exceed the liquid flow leaving the tank. The liquid flow rate from downcomer to active area is calculated based on the pressures at the downcomer bottom and active area bottom. In the flow, there is also a flow coefficient representing the head loss under the downcomer. In addition, in the vapor flow there is a flow coefficient representing the dry pressure drop. Values of the flow coefficients were defined based on the KG-TOWER result values of dry pressure drop and head loss under downcomer.

The model calculates the downcomer backup according to the total pressure drop, liquid height on the tray and head loss under the downcomer. Due to the configuration of the liquid flow from active area to downcomer, the liquid starts to accumulate on active area, if the downcomer if full. Thus, downcomer backup flooding occurs. Jet flooding flow and weeping flow as well as the maximum flow from the downcomer to the active area are calculated in the code according to the limit values and current vapor and liquid values. The set points for jet flooding and weeping flow rates are given at each time step according to the values of the correlations calculated in the code. The maximum liquid flow rate from the active area to the downcomer at a moment is set according to calculated value of the downcomer choke correlation. In Figure 5.17 the top, center and bottom part of the model are presented. In the figure, jet flooding lines are colored with red and weeping lines with blue. The flows that empty the active areas in weeping, when all the flows entering the active area are stopped, are colored with green. In addition, some controllers can be seen from the figure, but they are in manual mode, because the purpose of the distillation game is that the operator controls the valves according to his consideration.

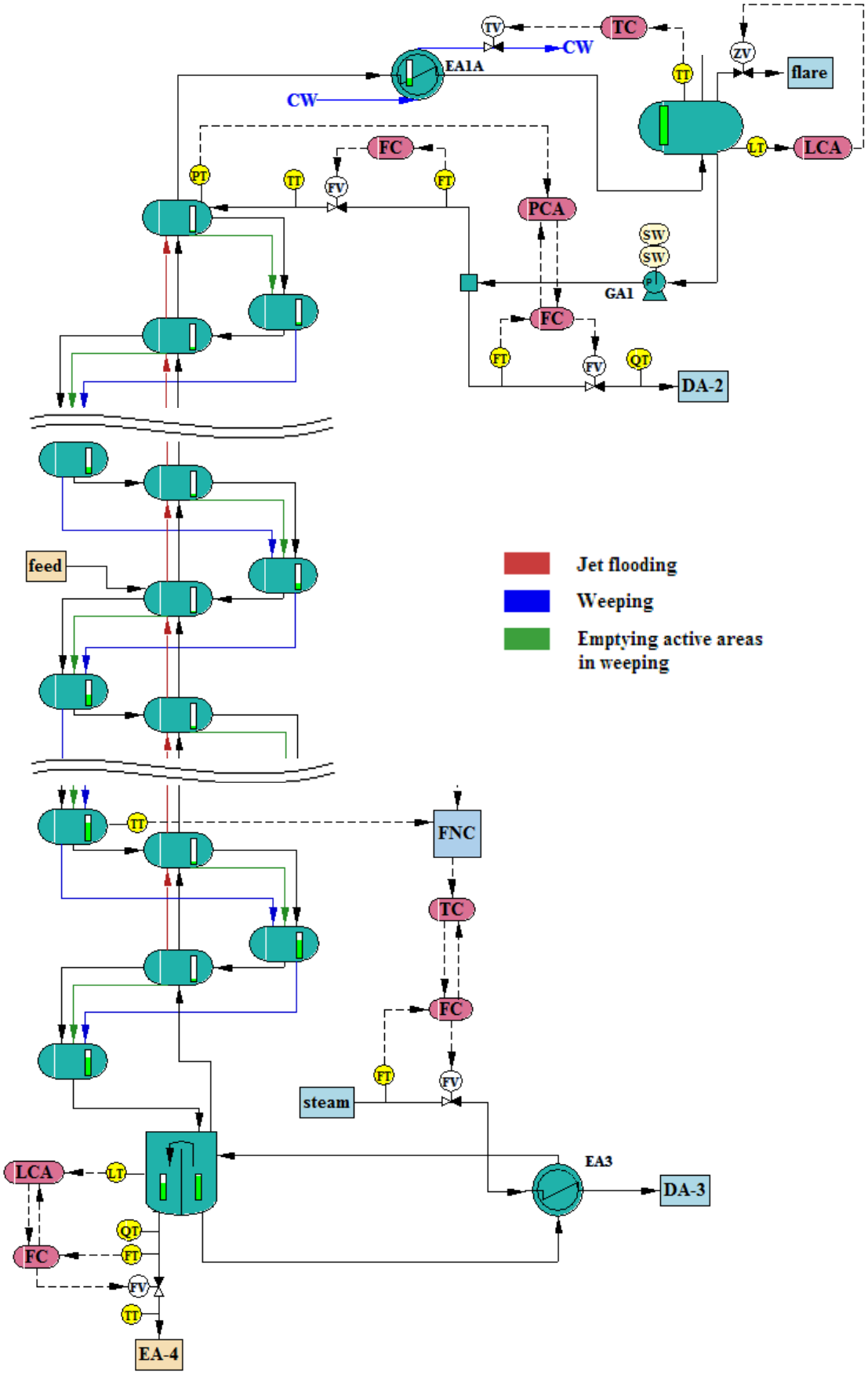

Figure 5.17. *Top, center and bottom part of the distillation column model.*

5.2.3 Simulation

After building and initializing the model, the model was run to steady-state first without occurring jet flooding, downcomer choke flooding and weeping. Dynamic distillation column models are often quite demanding to configure regarding the stability of the model. This particular distillation model, however, turned out to be very challenging, and finding the proper configuration took more time than expected. The pressure calculation in the condenser and the function of the reboiler seemed especially problematic. Pressures and vapor flow rates needed to be damped with pressure and flow filters. Nevertheless, even then, only small changes in the reboiler duty could be made to ensure the stability of the model. The flow rates, pressures, temperatures and composition of the distillate and bottom product were tried to get as near the corresponding of the original distillation game model as possible. However, some compromises needed to be done, since hydraulic limits were also considered and the normal operation of the column wanted to remain in the operation zone.

When the model remained stable in normal operation, the calculation of the hydraulic correlations was added to the model. It was soon noticed, that in the model the hydraulic phenomena do not occur as smooth as in the test case of the fixed pressure and couple of stirred tanks. There are many variables that interact with each other, i.e. in jet flooding when vapor flow is increased the entrainment liquid flow raises the levels of the tanks. That decreases the vapor flow, since the liquid accumulation increases the hydrostatic pressure and as the vapor flow also decreases jet flooding decreases. For this reason, the model is very difficult to get function smoothly and oscillation occurs easily in both flooding and in weeping. In the following, some simulation results of all the hydraulic phenomena are presented.

For examining jet flooding in the column, the reboiler duty was increased ramp-wise so that the vapor flow from the column base to the bottommost tray increased from 208 t/h to 374 t/h. In Figure 5.18 the vapor rate and in Figure 5.19 the liquid entrainment rate are presented as a function of the vertical column length at four different time steps. The lightest curves present the flows at the start time, the darker ones at certain time steps after that and the black curves present the flows at the latest time step. In Figure 5.18 the limit vapor flow value for jet flooding to occur is marked with orange dashed line for the top and the bottom part. The limit value for maximum jet flooding is marked with red dashed line. From Figures 5.18 and 5.19, it can be noticed that at the first, vapor flow is under the limit value of jet flooding and liquid entrainment rate is zero through the column, as in the normal operation. At the second captured time step, vapor flow is increased as the reboiler duty increases. Jet flooding occurs at almost all trays except trays 17…18 and 28…30. The reason why there is no jet flooding in these trays is that right above these trays there is a liquid accumulation, and thus there is no liquid flow to these trays. At the third captured time step, vapor rate reaches its maximum value and jet flooding increases. Because jet flooding causes liquid accumulation, and high

liquid levels on the trays increase the hydrostatic pressure, vapor flow starts to decrease despite that the reboiler duty remains at constant value. At the last captured time step, it can be observed that the vapor flow is decreased and jet flooding is almost totally stopped.

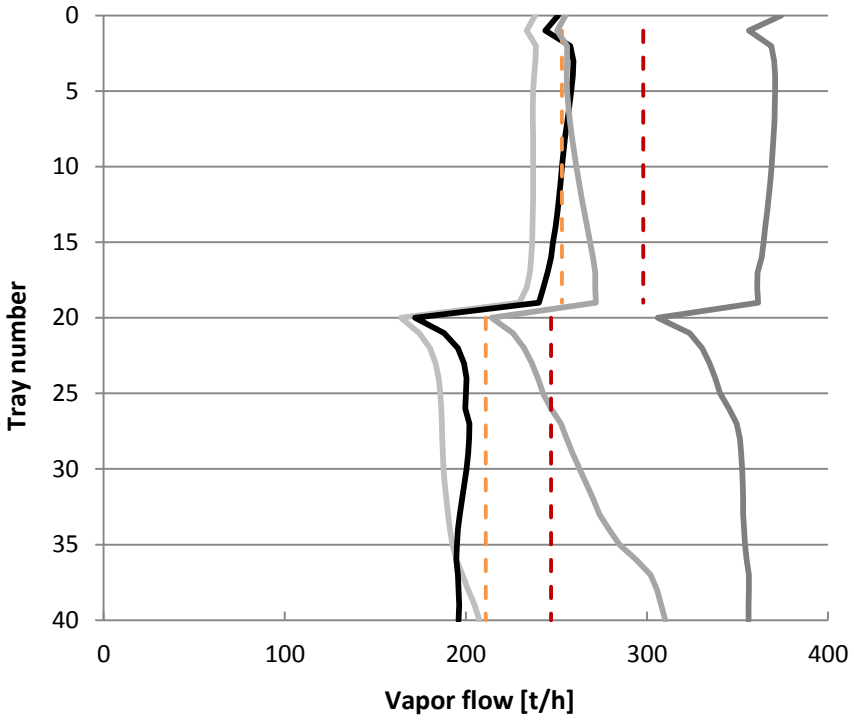

Figure 5.18. *Vapor flow rate through the column at four captured time steps.*

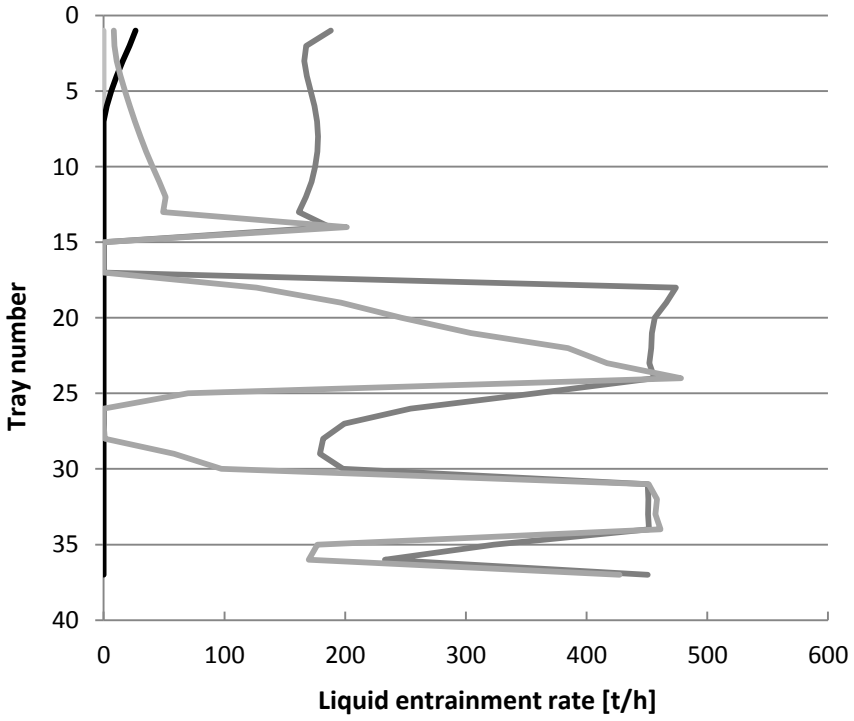

Figure 5.19. *Jet flooding through the column at four captured time steps.*

The downcomer choke flooding occurrence was examined by increasing the feed rate and then the reflux rate. The feed rate was increased ramp-wise from 312 t/h to 500 t/h and after a while the reflux rate was increased ramp-wise from 133 t/h to 218 t/h. In Figure 5.20 liquid flow rates from active areas to downcomers are presented as a function of the vertical column length at four different time steps. The limit value for downcomer choke effect to occur is marked in the figure with orange dashed line for the top and the bottom part. The limit value for maximum choke flow rate is marked with red dashed line. In Figure 5.21 liquid levels of the active areas are presented at the same time steps. The lightest curves present the flows and levels at the start time, the darker ones at certain time steps after that and the black curves present the flows and levels at the latest time step.

At the first time step, the feed and reflux rates are as in the normal operation. At the next captured time step, feed is increased. From Figure 5.20 can be seen, that the liquid flow rate from active area 20 to downcomer is restricted to its maximum value of 476.1 t/h. The flow rates in trays below the feed i.e. below tray 20 are approximately 450 t/h. Figure 5.21 shows that liquid starts to accumulate to tray 20 and the trays below. At the third captured time step reflux rate is also increased. It can be noticed, that now also the liquid rates in the top part of column become restricted. In addition, the liquid accumulation starts to occur in top of the column. In the last captured time step, feed and reflux are remained in constant value, but since there is a massive liquid accumulation in trays 10…19, the liquid flow starts to decrease.

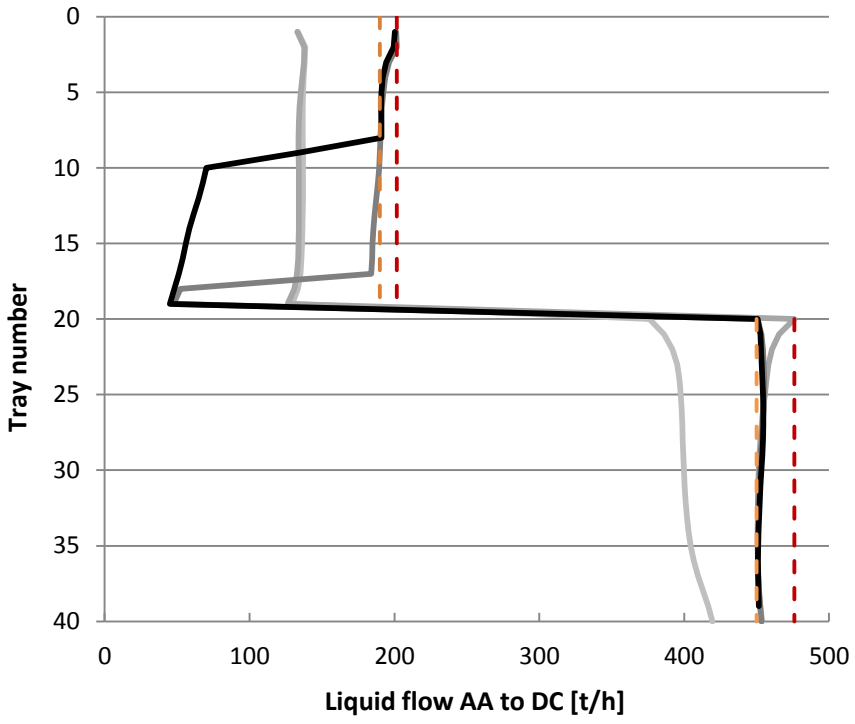

Figure 5.20. *Liquid flow rate from active areas to downcomers through the column.*

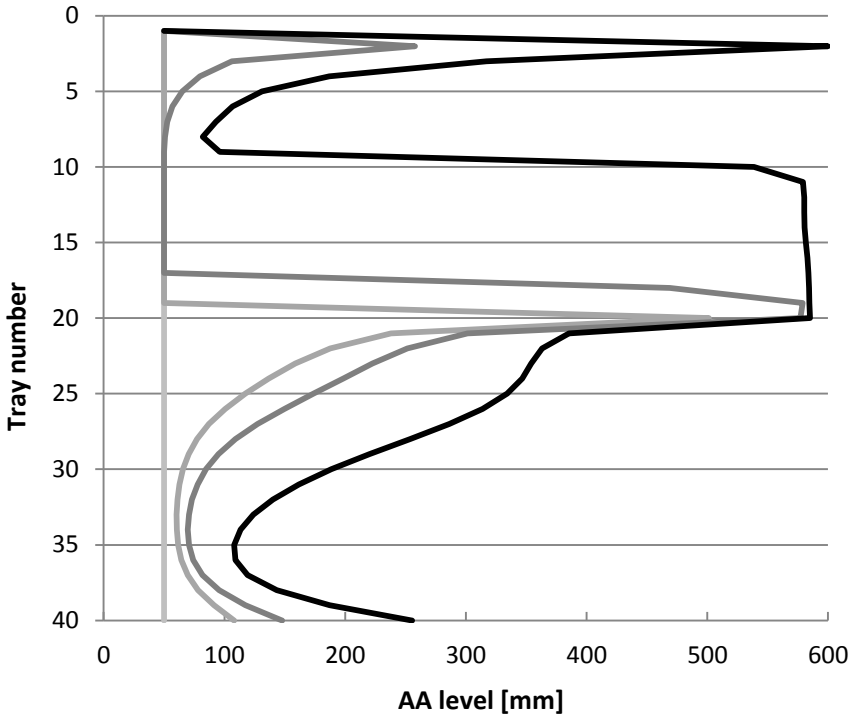

Figure 5.21. *Liquid levels of active areas at four captured time steps.*

Lastly, the weeping in the column was examined by decreasing the reboiler duty rampwise. The vapor flow from column base to the bottommost tray however started to oscillate after the reboiler duty was set to zero instead of remaining at value of zero. In order to observe weeping properly, the vapor flow rate was manipulated to be zero by adding a negative heat input to the column base after the reboiler duty was decreased to zero. In Figure 5.22 the vapor flow rates are presented as a function of the vertical column length at four different time steps. The limit value for weeping, 30 t/h, is marked in the figure with red dashed line. In Figure 5.23 the weeping liquid flow through the column are shown at the same time steps. The lightest curves present the flows at the start time, the darker ones at certain time steps after that, and the black curves present the flows at the latest time step.

At the first time step, the reboiler duty is in normal level and the vapor rate is high enough to prevent weeping. At the second captured time step, the reboiler duty is started to decrease and the vapor flow is under the limit value for weeping in trays 20...27 and thus weeping occurs at these trays. At the third captured time step, the reboiler duty is decreased to zero and vapor flow in all trays below the feed is zero. Since some of the liquid feed vaporizes in the tray 20, the vapor flow above it is still above the limit value. Weeping occurs below the tray 20 and as the vapor flow is zero, all liquid fed to the tray 20 weeps to the bottom. At the last captured time step the vapor flow from column base to bottom remains zero, but the feed is also stopped. Now the vapor flow through the column is under the limit value, and all the reflux fed to the topmost tray is wept through the column.

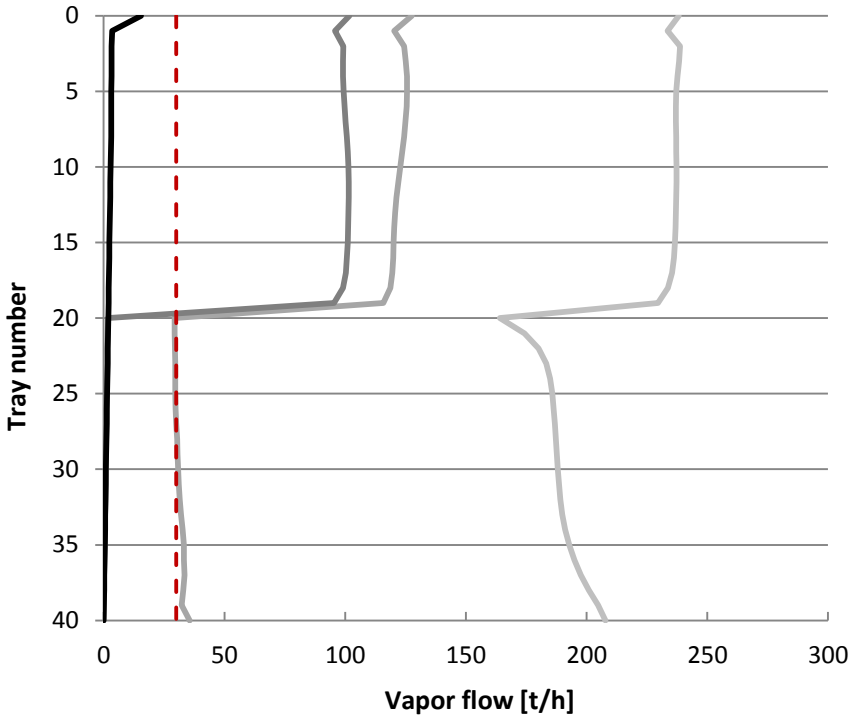

Figure 5.22. *Vapor flow rate through the column at four captured time steps.*

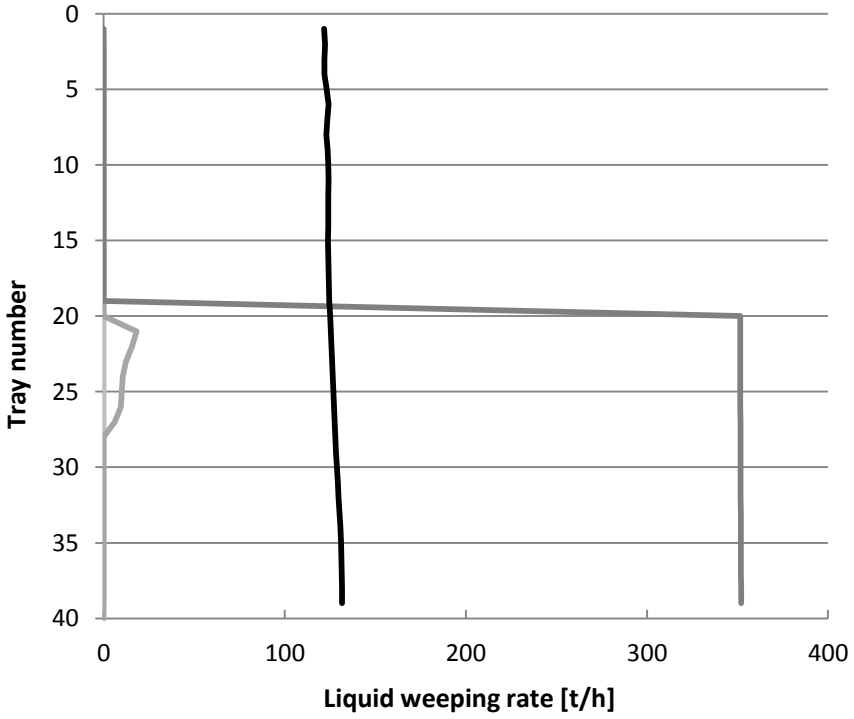

Figure 5.23. *Weeping through the column at four captured time steps.*

As the results presented above are only from few specific time steps, it is not possible to observe the function of the column through the whole simulation time. These results, however, give a good overview of the column function in the simulated cases.

6. RESULTS AND DISCUSSION

The objectives of this thesis was to examine and explain the tray hydraulics in the distillation column, describe the function of the current distillation model in the dynamic process simulator and develop an improved distillation model which takes into account the tray hydraulics. The hydraulic calculation was also purposed to implement in the dynamic process simulator by programming. The intention of the distillation model improvement was to utilize the model in operator training. With a distillation model of tray hydraulics, the operators could be trained to recognize when a distillation column is approaching or exceeding the hydraulic constraints. Thus, upset situations could be avoided and faster corrective actions to get the process back to the normal condition could be made by the operators.

6.1 Conclusions

The literature part of the thesis offered an overview of distillation columns and their internals as well as the hydraulic constraints of a tray column. The modelling of the hydraulic phenomena as jet flooding, downcomer backup flooding, downcomer choke flooding, weeping and foaming was studied. It was noticed that there is plenty of published information about the limit values for all hydraulic phenomena to occur. Nevertheless, there is very little information about the amounts of the liquid entrainment rate, limitation of the choke flow, liquid weeping rate and foaming. All the information found in the literature study, was utilized to rationalize the correlations for the hydraulic phenomena.

In the applied part of this thesis, the distillation model with hydraulic calculation was developed. The structure of the distillation model was changed to enable the hydraulic phenomena to occur in the model. As before in the distillation column model, each tray was modelled with one stirred tank, in the developed model, there was one tank representing the active area and one tank representing the downcomer. With a structure like that, it was possible to add flows in the model that enabled hydraulic phenomena as jet flooding, downcomer choke flooding and weeping to occur in the model. Downcomer backup flooding occurred in the model automatically due to the structure and the configuration of the model. Instead, the amount of jet flooding and weeping flows along with the maximum allowed flow of the downcomer choke effect was calculated based on the correlations. The calculation of the correlations was implemented in the dynamic simulator by programming.

Since the correlations found in the literature part were not straightforward and contained parameters that are difficult to determine, it was decided to utilize the tray manufacturer Koch-Glitsch's commercially available KG-TOWER software for defining the correlations for jet flooding, weeping and downcomer choke flooding. The software did not concern foaming in any way, and since there was very little information about modelling of the foaming available in the field's literature, it was decided not to include foaming in the model.

The KG-TOWER software did give as a result the limit values at which each hydraulic phenomenon begins. The values at which the maximum jet flooding and maximum downcomer choke flooding occurs could also be defined based on the results. Nevertheless, the software did not give any information about the amount of liquid entrained to the tray above in jet flooding nor the amount of liquid wept to the tray below in weeping. Neither did the software give any information about the value to which the liquid flow from the active area to the downcomer is limited. For that reason, the correlations were rationalized based on the information found in the literature study.

The maximum amount of entrained liquid was described to be all the liquid fed to the tray. The function between the limit value and maximum value was assumed to be linear, since there was no further information of that. In the extreme weeping, it was related that all liquid is wept and no liquid will flow through the downcomer. The vapor flow rate at which maximum weeping occurs was rationalized to be zero. The correlation for weeping was assumed to be linear between zero and the limit value of weeping.

For downcomer choke effect, it was described that as the as the frictional losses become excessive at the downcomer inlet, the normal weir flow is prevented and not all of the frothy mixture can be transported to the tray below. As there was not more specific information available, it was assumed that the flow is limited according to linear function if the liquid attempting to flow to the downcomer is between the limit value of choke effect to begin and the limit value of maximum downcomer choke flooding to occur. It was also hypothesized that after exceeding the limit value of maximum downcomer flooding the liquid flow is constant. The constant value at which the flow is restricted was decided to be 90 % of the limit value of maximum downcomer choke flooding. The value of 90 % was decided based on the fact that it needed to be more than the limit value of choke effect to begin to occur and less than the limit value of maximum choke flooding, since some restriction was known to occur in exceeding the first limit value, but the total limitation was supposed to occur after exceeding the limit value of maximum flooding.

The function of the developed model was first tested with a small test model of five separation elements and fixed pressure. The vapor and liquid flows were varied to observe the behavior of the hydraulic calculation in the model. The pressures, liquid levels and flows were also calculated manually with a spreadsheet and the simulation results

were compared to those. As expected, the simulation results corresponded to the manually calculated ones. After ensuring the hydraulic phenomena functioned in the model as expected, the hydraulic calculation was programmed into the dynamic process simulator with ANSI Common Lisp.

The validity of the developed hydraulic correlations could not be verified, since there was no point of comparison for those in the literature. Regardless, the function of jet flooding, downcomer choke flooding and weeping in the model was considered reasonable and the accuracy of them was sufficient considering the initial purpose of the model development, operator training.

For more extensive examination of the developed hydraulic calculation, it was decided to implement it in a distillation game model. The model was reconfigured and run to steady-state first without the hydraulic calculation. Finding the proper configuration was challenging and some pressure and flow filters needed to be added in the model. The model was able to get stable, but only small changes in the reboiler duty could be made to ensure the stability of the model.

After stabilizing the column model, the hydraulic calculation was added to the model. In the model the hydraulic phenomena did not occur as smooth as in the case of the fixed pressure and couple of stirred tanks. There are many variables that interact with each other and it was very difficult to get the model to function smoothly. Some oscillation occurred easily both in flooding and in weeping. However, all the hydraulic phenomena did occur in the model according to implemented calculation as planned.

In this thesis, fouling and coking were not taken into account in distillation modelling. Both are phenomena that occur in the distillation column over the time. Since the operator training simulator, which was the initial target of the developed model, is not used to simulate columns for months or years uninterrupted, fouling and coking was not considered relevant to the model.

6.2 Future work

The model built for the distillation game remains stable only if small changes are made with the reboiler duty. Some oscillation also occurs easily both in flooding and in weeping. Since, in the game, users can do very large changes, the model configuration needs further examination for ensuring the stability in the whole operating range regardless of the magnitude of the rate of change.

The distillation model developed in this thesis concerns only tray columns. Packed columns differ quite much from tray columns, and the modelling of them would be a different case. Nevertheless, it would be advantageous to develop a distillation model that

also takes into account hydraulic phenomena in the packed column, since in the operator training simulators there are numerous packed columns.

As intended, the hydraulic calculation was implemented in the dynamic process simulator by programming ANSI Common Lisp. However, the user of the model would benefit if a user interface would have been created. The required values, defined based on the KG-TOWER results, have to be entered to the model manually for all lines separately; although, some simple programmatic commands can be utilized to enter the needed information to several lines at once. With a user interface, defining and changing the limit values for correlations could be faster and simpler.

In ProsDS, there is a standard distillation column model for the current column model. The model can be created and initialized easily with the initialization menu. Programming a same kind of initialization menu also for the developed column model would make the adding and configuration of the model easier and faster.

7. CONCLUSION

The need of maximizing the economic benefits of a distillation unit very often requires operating close to its capacity limits. The limits of an operating column depend on the internal vapor and liquid flows and their physical properties. The aim of this thesis was to improve distillation modelling in an in-house dynamic process simulator, ProsDS, to consider internal phenomena in a distillation column i.e. tray hydraulics. The purpose of the model improvement was to utilize it the in the training simulators.

The improved distillation model can provide beneficial support for operator training, in addition to theoretical training, considering the inner phenomena of a distillation column. With the improved model, it is possible to train operators to recognize the hydraulic constraints of a distillation column. Consequently, upset situations can be avoided and a process can be operated faster back to the normal condition. The model also offers a possibility to examine the internal vapor and liquid flows of a distillation column. This is a great advantage, since internal flows cannot be measured in a real column and thus it is difficult to obtain information about the inner phenomena of a distillation column.

In the literature part of the thesis, distillation columns and their internals as well as hydraulic constraints of a tray column were discussed. Modelling of the hydraulic phenomena as jet flooding, downcomer backup flooding, downcomer choke flooding, weeping and foaming was studied. It was noticed that there is plenty of information available in literature about determining the limit values for liquid and vapor rates, but very little information about the amounts of the liquid entrainment rate, limitation of the choke flow and liquid weeping rate.

In the applied part, the structure of the original distillation model was first reconsidered. Instead of one flash separator representing each tray, separate flash separators were used to represent an active area and a downcomer of a tray. The hydraulic phenomena that were decided to include in the model were jet flooding, downcomer backup flooding, downcomer choke flooding and weeping. Downcomer backup flooding occurred in the model automatically due to the model structure and configuration. For representing the other hydraulic phenomena correlations were used. These correlations were rationalized based on the literature study. For determining the limit values for each phenomenon to begin, and for maximum jet flooding and downcomer choke flooding to occur, Koch-Glitsch's KG-TOWER software was utilized.

The developed distillation model was first implemented in the dynamic process simulator with fixed pressure, and jet flooding, downcomer choke flooding and weeping oc-

curring on only one tray. The function of all the phenomena was tested by varying vapor and liquid flows in the model. The liquid flow rates, pressures and levels of the tanks were also calculated manually with a spreadsheet, and simulation results were compared to those to verify the accuracy of the simulation model. After ensuring the reasonable function of the correlation, the calculation of the correlations was implemented in the ProsDS by programming ANSI Common Lisp.

For more extensive examination, the model was implemented in a distillation game model. The model was first stabilized without hydraulic phenomena. After finding the proper configuration, hydraulic calculation was added to the model. The function of the model was studied by varying the reboiler duty, feed rate and reflux rate.

The simulation results showed that some oscillation occurs easily both in flooding and in weeping. Further examination of the model configuration is needed for ensuring the stability of the model when used in a training simulator or the distillation game. All the hydraulic phenomena did, however, occur in the model according to implemented calculation as assumed.

REFERENCES

[1] P. B. Desphande, Distillation Dynamics and Control, Instrument Society of America, New York, 1985, 513 p.

[2] M. Mecklin, K. Malila, P. Tuomikoski, J. Rousu, E. Tamminen, M. Pakarinen & J. Harju, Tislauksen perusteet, Neste Oil, Porvoo, 2009, 74 p.

[3] A. Brambilla, Distillation Control and Optimization, McGraw-Hill Education, USA, 2014, 393 p.

[4] P. S. Bucley, W. L. Luyben, & J. P. Shunta, Design of Distillation Column Control Systems, Instrument Society of America, USA, 1985, 532 p.

[5] J. Harju, PROSimulator Osa 1 Johdanto, Neste Jacobs Oy, Porvoo, 2007.

[6] J. Harju PROSimulator Osa 2.1 Prosessi, Neste Jacobs Oy, Porvoo, 2007.

[7] H. Tu & I. H. Rinard, ForeSee − A hierarchical dynamic modeling and simulation system of complex processes, Computers and Chemical Engineering, Vol. 30 (9), 2006, pp. 1324−1345.

[8] V. Kulikova, H. Briesena, R. Groscha, A.Yanga, L. von Wedelb & W. Marquardta, Modular dynamic simulation for integrated particulate processes by means of tool integration, Chemical Engineering Science, Vol. 60, 2005, pp. 2069−2083.

[9] Aspen Technology, Aspen Plus Dynamics, 2015. Available (accessed on 25.11.2015): https://www.aspentech.com/products/engineering/aspen-plus-dynamics/

[10] Aspen Technology, Aspen HYSYS Dynamics, 2015. Available (accessed on 25.11.2015): https://www.aspentech.com/products/engineering/aspen-hysys-dynamics/

[11] A. Lakshmanan & A. Rao, Jump Start: Using Aspen HYSYS Dynamics with Columns, Aspen Technology, 2015, 17 p.

[12] Chemstations, CHEMCAD Version 6 User Guide, 2007, 189 p. Available (accessed on 24.11.2015): http://www.chemstations.net/content/documents/CHEMCAD_6_User_Guide_-_online.pdf

[13] Process Systems Enterprise Limited, The gPROMS platform, 2013. Available (accessed on 25.11.2015): http://www.psenterprise.com/gproms/platform.html

[14] B. Chang, S. Lee, H. Kwon & I. Moon, Rigorous industrial dynamic simulation of a crude distillation unit considered valve tray rating parameters, Computers and Chemical Engineering, Vol. 22 (Supplement 1), 1998, pp. 863−866.

[15] H. Z. Kister, Distillation Operation, McGraw-Hill, USA, 1990, 729 p.

[16] C. D. Holland, Fundamentals of Multicomponent Distillation, 7th Edition, McGraw-Hill, New York, 1981, 626 p.

[17] Separation Technologies, Distillation Column Tray Selection & Sizing, 2016. Available (accessed on 14.5.2016): http://seperationtechnology.com/distillation-column-tray-selection-1

[18] Separation Processes, Column Internals, 2015. Available (accessed on 11.12.2015): http://www.separationprocesses.com/Operations/POT_Chp02.htm

[19] Tislaus, KE-42.3100 Kemian laitetekniikka IIa, Lecture material, 2009, 42 p.

[20] R. Billet, Distillation Engineering, Chemical Publishing Co., New York, 1979, 519 p.

[21] R.H. Perry & D. W. Green, Perry's Chemical Engineers' Handbook, 8th Edition, McGraw-Hill, USA, 1999.

[22] M. J. Locket, Distillation Tray Fundamentals, Cambridge University Press, Cambridge, 1986, 226 p.

[23] J. Ingham, I. J. Dunn, E. Heinzle, J. E. Přenosil & J. B. Snape, Chemical Engineering Dynamics: An Introduction to Modelling and Computer Simulation, 3th Edition, Wiley-VCH, Weinhelm, 2007, 618 p.

[24] Ű. Can, M. Jimoh, J. Steinbach & G. Wozny, Simulation and experimental analysis of operational failures in a distillation column, Separation and Purification Technology, Vol. 29 (2), 2002, pp. 163−170.

[25] B. Wittgens & S. Skogestad, Evaluation of Dynamic Models of Distillation Columns with Emphasis on the Initial Response, DYCORD +95, Helsingør, Denmark, June 7−9, 1995.

[26] J. R. Fair, Design of Equilibrium State Processes, McGraw-Hill, USA, 1963, Chapter 15.

[27] Glitsch, Ballast Tray Design Manual, Glitsch Inc., Dallas, 1974.

[28] Koch Engineering Co, Flexitray Design Manual, Koch Engineering Co. Inc., Wichita, Kansas, 1982.

[29] Nutter Engineering Co, Float Valve Design Manual, Nutter Engineering Co., Tulsa, Oklahoma, 1976.

[30] K. Ruff, T. Pilhofer & A. Mersmann, Ensuring flow through all the openings of perforated plates for fluid dispersion, International Journal of Chemical Engineering, Vol. 18 (3), pp. 395−401.

[31] A. Górak & H. Schoenmakers, Distillation: Operation and Applications, Academic Press, 2014, 450 p.

[32] Koch-Glitsch, Introduction to KG-TOWER, 2006. Available (accessed on 30.12.2015): http://www.nt.ntnu.no/users/skoge/prost/proceedings/distillation10/DA2010%20Sponsor%20Information/Koch%20Glitsch/KGTower/IntroKGTowerV2.0.pdf

APPENDIX A: KG-TOWER RESULTS FOR TEST CASE

KOCH-GLITSCH®

KG-TOWER® Software v 5.2

Customer's copy.

Strictly confidential. Property of Koch-Glitsch.

Registered To: Tuuli Seppänen, Neste Jacobs

VALVE TRAY RATING DATA

Project Name	Master's Thesis		Date :	15-Mar-2016	Page : 1
Tower Name	DA-10203		File :	DA-10203_TOP_kaikki.kgt	
Case Name	Tray Hydraulics		By :	seppatuu	Revision : 1

ZONE		Top	Top	Top	Top
DESCRIPTION		60%	80%	100%	120%
TRAY NUMBER		2-15	2-15	2-15	2-15
% OF LOADING		100	100	100	100
LOADINGS					
Vapor Rate	kg/hr	132978	177304	221630	265956
Vapor Density	kg/m3	5,470	5,470	5,470	5,470
Vapor Volume	m3/s	6,75	9,00	11,25	13,51
Vapor Viscosity	cP	0,0083*	0,0083*	0,0083*	0,0083*
Liquid Rate	kg/hr	77049	102732	128415	154099
Liquid Density	kg/m3	629,86	629,86	629,86	629,86
Liquid Volume	m3/hr	122,33	163,10	203,88	244,65
Surface Tension	mN/m	12,97	12,97	12,97	12,97
Liquid Viscosity	cP	0,209	0,209	0,209	0,209
* Calculated from other physical properties.					
Tray Spacing	mm	600,00	600,00	600,00	600,00
System Factor		1,00	1,00	1,00	1,00
Jet Flood	%	53	69	86	104
Downcomer Flood	%	35	46	58	69
Downcomer Backup	mm liq	126,5	161,8	206,9	266,4
Downcomer Exit Velocity	m/s	0,228	0,304	0,381	0,457
Dry Tray Pressure Drop	mm liq	38,8	68,1	105,4	150,6
Total Tray Pressure Drop	mm liq	78,3	107,2	144,1	191,1
Total Tray Pressure Drop	mm Hg	3,6	5,0	6,7	8,9
Cf Active Area	m/s	0,07	0,09	0,11	0,14
Weir Load	m3/h/m	32,9	43,8	54,8	65,8
Weir Crest	mm liq	29,0	35,2	40,8	46,1
Downcomer Backup	% (TS+W)	19,5	24,9	31,8	41,0
Head Loss Under DC	mm liq	8,3	14,8	23,1	33,2
DC Residence Time	sec	12,2	9,1	7,3	6,1
DC Loading	m3/hr/m2	192,1	256,2	320,2	384,3
Blow Rating	%	52	69	N/A	N/A
System Limit	%	41	55	68	81
Turndown	%	60	45	36	30
Unit Reference	%	125	167	209	251
Equation 13	%	55	73	91	110
WARNINGS:				1,	1,2,

WARNINGS:

1. Jet flood exceeds design limit.
2. Excessive dry tray pressure drop. Try increased valve quantity, more open area or increased tray spacing.
3. Top side downcomer chord length is less than 55% of diameter. Use a larger side downcomer.
4. Bottom side downcomer edge length is less than 55% of diameter. Tray efficiency may be affected.

APPENDIX B: SPREADSHEET CALCULATIONS (1/2)

Area AA [m^2]		9.31	Time		
Area DC [m^2]		0.64	2.9667	2.9700	2.9733
AA-2	level [mm]		50.0000	50.0000	50.0000
	pressure [kPa]		180.8969	180.8969	180.8969
	pressure difference [kPa]		0.3145	0.3145	0.3145
	bottom pressure [kPa]		181.2114	181.2114	181.2114
	density [kg/m3]		641.2413	641.2417	641.2423
AA-2 to DC-2	flow [t/h]		127.8413	128.0579	128.3175
DC-2	level [mm]	$h_t = h_{t-1} + (L_{t-1}^{in} - L_{t-1}^{out})/(3.6 * \rho A_{DC}) * \Delta t * 1000$	214.5780	214.6067	215.8220
	pressure [kPa]	$p = p_{AA-2}$	180.8969	180.8969	180.8969
	pressure difference [kPa]	$\Delta p = \rho g h$	1.3498	1.3500	1.3576
	bottom pressure [kPa]	$p_{bot} = p + \Delta p$	182.2467	182.2469	182.2545
DC-2 to AA-3 LIQUID	flow [t/h]	$Q = K_v * \sqrt{\Delta p}/\sqrt{\rho/\rho_{water}}$	127.6299	119.0800	129.8236
	h_{udc} [kPa]	$\Delta p = \frac{Q^2 * \rho/\rho_{water}}{K_v^2}$	0.1411	0.1254	0.1490
AA-3	level [mm]	$h_t = h_{t-1} + (L_{t-1}^{in} - L_{t-1}^{out})/(3.6 * \rho A_{AA}) * \Delta t * 1000$	50.0000	49.9895	49.9941
	pressure [kPa]	$p = p_{AA-2} + dp_{dry}$	181.7927	181.8087	181.7927
	pressure difference [kPa]	$\Delta p = \rho g h$	0.3129	0.3128	0.3128
	bottom pressure [kPa]	$p_{bot} = p + \Delta p$	182.1056	182.1215	182.1055
	density [kg/m3]		637.8657	637.8658	637.8659
AA-3 to AA-2 VAPOR	flow [t/h]		216.4161	217.0322	217.0323
	dp_{dry} [kPa]	$\Delta p = \frac{Q^2 * \rho/\rho_{water}}{K_v^2}$	0.5813	0.5973	0.5973
	density [kg/m3]		5.1847	5.1847	5.1847
AA-3 to DC-3	flow [t/h]	$L_t^{out} = L_t^{in} + \frac{h_t - h_{t-1}}{1000} * 3.6 * A_{AA} * \rho/\Delta t$	128.0838	117.9542	130.3224
DC-3	level [mm]	$h_t = h_{t-1} + (L_{t-1}^{in} - L_{t-1}^{out})/(3.6 * \rho A_{DC}) * \Delta t * 1000$	215.3267	215.3272	214.9638
	pressure [kPa]	$p = p_{AA-3}$	181.7927	181.8087	181.7927
	pressure difference [kPa]	$\Delta p = \rho g h$	1.3474	1.3474	1.3451
	bottom pressure [kPa]	$p_{bot} = p + \Delta p$	183.1401	183.1561	183.1378
DC-3 to AA-4 LIQUID	flow [t/h]	$Q = K_v * \sqrt{\Delta p}/\sqrt{\rho/\rho_{water}}$	128.0799	120.6247	125.7229
	h_{udc} [kPa]	$\Delta p = \frac{Q^2 * \rho/\rho_{water}}{K_v^2}$	0.1427	0.1293	0.1405
AA-4	level [mm]	$h_t = h_{t-1} + (L_{t-1}^{in} - L_{t-1}^{out})/(3.6 * \rho A_{AA}) * \Delta t * 1000$	50.0000	49.9954	49.9971
	pressure [kPa]	$p = p_{AA-3} + dp_{dry}$	182.6853	182.7148	182.6853
	pressure difference [kPa]	$\Delta p = \rho g h$	0.3121	0.3120	0.3120
	bottom pressure [kPa]	$p_{bot} = p + \Delta p$	182.9974	183.0268	182.9974
	density [kg/m3]		636.2181	636.2181	636.2181
AA-4 to AA-3 VAPOR	flow [t/h]		216.8703	217.0322	217.0323
	dp_{dry} [kPa]	$\Delta p = \frac{Q^2 * \rho/\rho_{water}}{K_v^2}$	0.5798	0.5932	0.5932
	density [kg/m3]		5.2202	5.2202	5.2202

APPENDIX B: SPREADSHEET CALCULATIONS (2/2)

AA-4 to AA-3	flow [t/h]	0.0000	0.0000	0.0000
AA-4 to DC-4	flow [t/h] $\mathrm{L_t^{out}} = L_t^{in} + \frac{h_t - h_{t-1}}{1000} * 3.6 * A_{AA} * \rho / \Delta t$	128.2414	120.1324	125.9037
DC-3 to DC-4	flow [t/h]	0.0000	0.0000	0.0000
DC-4	level [mm] $h_t = h_{t-1} + (L_{t-1}^{in} - \mathrm{L_{t-1}^{out}})/(3.6 * \rho A_{DC}) * \Delta t * 1000$	215.4392	215.4398	215.2928
	pressure [kPa] $p = p_{AA-4}$	182.6853	182.7148	182.6853
	pressure difference [kPa] $\Delta p = \rho g h$	1.3446	1.3446	1.3437
	bottom pressure [kPa] $p_{bot} = p + \Delta p$	184.0300	184.0594	184.0290
DC-4 to AA-5 LIQUID	flow [t/h] $Q = K_v * \sqrt{\Delta p} / \sqrt{\rho / \rho_{water}}$	128.2372	121.2093	126.4732
	h_{udc} [kPa] $\Delta p = \frac{Q^2 * \rho / \rho_{water}}{K_v^2}$	0.1434	0.1309	0.1425
AA-5	level [mm] $h_t = h_{t-1} + (L_{t-1}^{in} - \mathrm{L_{t-1}^{out}})/(3.6 * \rho A_{AA}) * \Delta t * 1000$	50.0000	50.0000	50.0000
	pressure [kPa] $p = p_{AA-4} + dp_{dry}$	183.5746	183.6166	183.5746
	pressure difference [kPa] $\Delta p = \rho g h$	0.3119	0.3119	0.3119
	bottom pressure [kPa] $p_{bot} = p + \Delta p$	183.8866	183.9285	183.8865
	density [kg/m3]	635.8866	635.8866	635.8866
AA-5 to AA-4 VAPOR	flow [t/h]	217.0320	217.0322	217.0323
	dp_{dry} [kPa] $\Delta p = \frac{Q^2 * \rho / \rho_{water}}{K_v^2}$	0.5772	0.5898	0.5898
	density [kg/m3]	5.2509	5.2509	5.2509

APPENDIX C: KG-TOWER RESULTS FOR DISTILLATION GAME MODEL TOP PART (1/2)

KOCH-GLITSCH®
KG-TOWER® Software v 5.2
Registered To: Tuuli Seppänen, Neste Jacobs

Customer's copy.
Strictly confidential. Property of Koch-Glitsch.

VALVE TRAY RATING DATA

Project Name	Master's Thesis		Date :	16-Mar-2016	Page : 1
Tower Name	DA-10203		File :	Tislauspeli_TOP.kgt	
Case Name	Tray Hydraulics		By :	seppatuu	Revision : 1

ZONE		Top	Top	Top	Top
DESCRIPTION		60%	80%	100%	120%
TRAY NUMBER		1-19	1-19	1-19	1-19
% OF LOADING		100	100	100	100
LOADINGS					
Vapor Rate	kg/hr	132978	177304	221630	265956
Vapor Density	kg/m3	5,470	5,470	5,470	5,470
Vapor Volume	m3/s	6,75	9,00	11,25	13,51
Vapor Viscosity	cP	0,0083*	0,0083*	0,0083*	0,0083*
Liquid Rate	kg/hr	77049	102732	128415	154099
Liquid Density	kg/m3	629,86	629,86	629,86	629,86
Liquid Volume	m3/hr	122,33	163,10	203,88	244,65
Surface Tension	mN/m	12,97	12,97	12,97	12,97
Liquid Viscosity	cP	0,209	0,209	0,209	0,209
* Calculated from other physical properties.					
Tray Spacing	mm	600,00	600,00	600,00	600,00
System Factor		1,00	1,00	1,00	1,00
Jet Flood	%	53	71	89	107
Downcomer Flood	%	20	27	34	41
Downcomer Backup	mm liq	113,8	144,1	186,0	245,1
Downcomer Exit Velocity	m/s	0,112	0,149	0,186	0,224
Dry Tray Pressure Drop	mm liq	41,2	73,3	114,5	164,8
Total Tray Pressure Drop	mm liq	76,3	106,6	146,9	200,2
Total Tray Pressure Drop	mm Hg	3,5	4,9	6,8	9,3
Cf Active Area	m/s	0,08	0,10	0,13	0,15
Weir Load	m3/h/m	27,4	36,5	45,6	54,7
Weir Crest	mm liq	25,7	31,1	36,1	40,8
Downcomer Backup	% (TS+W)	17,5	22,2	28,6	37,7
Head Loss Under DC	mm liq	2,0	3,5	5,5	8,0
DC Residence Time	sec	20,8	15,6	12,5	10,4
DC Loading	m3/hr/m2	112,7	150,2	187,8	225,3
System Limit	%	41	55	68	81
Unit Reference	%	106	142	177	213
Equation 13	%	60	81	101	121
WARNINGS:				1.	1,2.

WARNINGS:
1. Jet flood exceeds design limit.
2. Excessive dry tray pressure drop. Try increased valve quantity, more open area or increased tray spacing.

APPENDIX C: KG-TOWER RESULTS FOR DISTILLATION GAME MODEL BOTTOM PART (2/2)

KOCH-GLITSCH®

KG-TOWER® Software v 5.2

Registered To: Tuuli Seppänen, Neste Jacobs

Customer's copy.
Strictly confidential. Property of Koch-Glitsch.

VALVE TRAY RATING DATA

Project Name	Master's Thesis		**Date :**	16-Mar-2016	**Page :** 1
Tower Name	DA-10203		**File :**	Tislauspell_BOTTOM.kgt	
Case Name	Tray hydraulics		**By :**	seppatuu	**Revision :** 1

ZONE		Bottom	Bottom	Bottom	Bottom
DESCRIPTION		60%	80%	100%	120%
TRAY NUMBER		20-40	20-40	20-40	20-40
% OF LOADING		100	100	100	100
LOADINGS					
Vapor Rate	kg/hr	106929	142572	178215	213858
Vapor Density	kg/m3	6,087	6,087	6,087	6,087
Vapor Volume	m3/s	4,88	6,51	8,13	9,76
Vapor Viscosity	cP	0,0086	0,0086	0,0086	0,0086
Liquid Rate	kg/hr	244348	325798	407247	537566
Liquid Density	kg/m3	640,41	640,41	640,41	640,41
Liquid Volume	m3/hr	381,55	508,74	635,92	839,41
Surface Tension	mN/m	13,01	13,01	13,01	13,01
Liquid Viscosity	cP	0,209	0,209	0,209	0,209
Tray Spacing	mm	600,00	600,00	600,00	600,00
System Factor		1,00	1,00	1,00	1,00
Jet Flood	%	49	65	81	99
Downcomer Flood	%	36	49	61	80
Downcomer Backup	mm liq	172,2	211,3	276,8	369,6
Downcomer Exit Velocity	m/s	0,319	0,425	0,531	0,702
Dry Tray Pressure Drop	mm liq	40,3	54,7	85,4	123,0
Total Tray Pressure Drop	mm liq	97,9	118,2	157,9	206,1
Total Tray Pressure Drop	mm Hg	4,6	5,6	7,4	9,7
Cf Active Area	m/s	0,06	0,08	0,10	0,12
Weir Load	m3/h/m	74,1	98,8	123,5	163,0
Weir Crest	mm liq	49,9	60,5	70,2	84,4
Downcomer Backup	% (TS+W)	26,5	32,5	42,6	56,9
Head Loss Under DC	mm liq	16,2	28,8	45,0	78,4
DC Residence Time	sec	8,9	6,6	5,3	4,0
DC Loading	m3/hr/m2	204,2	272,3	340,3	449,2
System Limit	%	31	41	52	64
Unit Reference	%	83	110	138	165
Equation 13	%	61	82	102	126
WARNINGS:					1,2,3,4,

WARNINGS:

1. Jet flood exceeds design limit.
2. Excessive downcomer backup. Try increased downcomer clearance, lower weir height, increased % open area or increased quantity of valves.
3. Excessive dry tray pressure drop. Try increased valve quantity, more open area or increased tray spacing.
4. Excessive downcomer exit velocity. Try increased downcomer clearance.